Supplementary Material

A Circular Dichroism – DFT Method for Conformational Study of Flexible Molecules: the Case of 1- and 2-Naphthyl Diesters

Marcin Kwit, Natalia Prusinowska, Robert Cysewski, Beata Warżajtis, Urszula Rychlewska, and Jacek Gawroński

Adam Mickiewicz University, Department of Chemistry, Umultowska 81B, 61 614 Poznan, Poland
E-mail: marcin.kwit@amu.edu.pl, urszular@amu.edu.pl, gawronsk@amu.edu.pl

Table of Contents

X-Ray studies

Crystals of **6a** and **6b**, suitable for X-ray diffraction analysis, were obtained by slow evaporation from dichloromethane/*n*-hexane solution. The most relevant crystal and refinement data are collected in Table I1 of the Supporting Information. Single crystal X-ray diffraction data were collected on a SuperNova CCD diffractometer equipped with Cu Kα radiation. The measurements were first performed at room temperature but for the α-naphtol derivative (**6a**) additional data collection has been performed at 150K. Both room and low temperature data sets for (**6a**) indicated a nearly whole molecule disorder around the two-fold symmetry axis in $P3_221$ space group, with one carbon atom of the cyclopropane ring on site symmetry **3b**. At this point we have faced the following ambiguity in interpreting the disorder model. Either the formally C_2 symmetric molecule utilizes this symmetry in crystal but adopts two partially and unevenly occupied orientations, or the molecule in crystal adopts the C_1 symmetry but in spite of this it is situated on a two-fold symmetry axis. The latter interpretation requires 50:50% occupancy of the two symmetry two-fold related sites. The answer which of the two models is more reliable came from the analysis of the data deposited in the CSD[1]. We have searched for cyclopropane substituted at C1 and C2 by $C_{sp}{}^2$ carbon atoms using filters no-disorder, no-powder, R<7.5%. Among 14 crystal structures containing chiral cyclopropane ring the 18 values of the $C_{sp}{}^2$–$C_{sp}{}^3$–$C_{sp}{}^3$– $C_{sp}{}^2$ torsion angle magnitude covered a narrow range of 133.5 to 144.9°. The observation was confirmed by quantum chemical calculations. The average value of the $C_{sp}{}^2$–$C_{sp}{}^3$–$C_{sp}{}^3$– $C_{sp}{}^2$ torsion angle moduli in six low-energy conformers amounts to 142.3(1.7)º (Table H1). To achieve similar value in our model structure we had to assume that the molecule in crystal possesses non-symmetrical conformation but is nonetheless situated on a two-fold symmetry axis. Therefore the occupancy ratio of the two sites has to be 50:50. Unfortunately, the assumption of the equal occupancy of the two positions yielded noticeably different atomic displacement parameters in the two parts of one molecule. Therefore, we have lowered the crystal symmetry to $P3_2$ assuming the presence of the merohedral twinning. The twin law (0 1 0 1 0 0 0 0 −1) corresponded to the twofold operation that is present in the apparent Laue group, but not in the true space group. Lowering the crystal symmetry had no effect on the disorder but allowed us to reasonably model the molecular conformation and the partial occupancy of the two alternative positions, which refined to values 0.54:0.46. Due to the presence of disorder it became necessary to apply in the refinement process the rigid group constrains for the naphthalene moieties (AFIX 167) and restrains on displacement parameters (SIMU 0.04). Data collection strategy, data reduction and cell refinement were performed with the program *CrysAlisPRO*.[2] The intensity data were corrected for Lp effects. The structures were solved by direct methods using *SHELXS86*[3] and refined by least-squares techniques with *SHELXL-2014/7*.[4] For all non-hydrogen atoms anisotropic displacement parameters were employed. The positions of the hydrogen atoms were calculated at standardized distances and were refined using a riding model with the distance constraints depending on the temperature at which the X-ray measurements have been carried out, i.e. C(phenyl)–H=0.95, methine C(sp^3)–H=1.00 and methylene C(sp^3)–H=0.99Å [U_{iso}(H) = 1.2U_{eq}(C)] for the crystal structure of **10a** determined at 150K, and C(phenyl)–H=0.93, methine C(sp^3)–H=0.98 and methylene C(sp^3)–H=0.97Å [U_{iso}(H) = 1.2U_{eq}(C)] for the crystal structure of **6b** determined at 295 K. The absolute structure of the crystals could not be determined solely on the basis of the X-ray data, for the Flack parameter[5] was inconclusive. The final confirmation of the correctly determined absolute structure of crystals **6a** and **6b** arose from comparison of molecular configuration obtained from X-ray structure with the absolute configuration of the substrates, which was (1*S*, 2*S*).

Figures were prepared using Mercury[6] program.

X-Ray diffraction study of 6b

Diester **6b** crystallizes in $P2_1$ space group with two symmetry independent molecules of C_1 symmetry. The two molecules differ mainly in the *anti/syn* orientation of the C–O bond with respect to the cyclopropane C–C bond, described in Figure 2 by a set of the γ-angles, which adopt the values of -157.2(4) and -166.7(4) in one molecule, and 15.0(5) and 29.0(6)º in the other molecule. Both molecules possess the same (*S,S*) chirality at the stereogenic centers. Unlike in **6a**, the two naphthyl groups in **6b** are nearly parallel forming angles of 8.3 and 17.4° (Figure A2).

In all crystallographically characterized molecules one can distinguish several pairs of either C=O or C–O bonds that lie nearly parallel to the C–H dipoles situated in relative 1,3-positions, which suggest the presence of stabilizing local CO/CH dipole/dipole interactions.

Computational details

It is well-documented that the conformation of a molecule has a substantial influence on its physical and chemical properties.[7] Thus, reliable conformational analysis is of critical importance for arriving at computational results close to the experimental ones. It has been shown that even minor changes in molecule conformation can result in a change of sign and/or magnitude of the calculated chiroptical properties.[8] For generation of all possible conformers of the molecule in question, the Monte Carlo search or systematical conformational search with the use of common force field methods is the most frequently used solution. In the latter case, the number of possible conformers grows rapidly with the increase of variables such as the number of torsion angles or other structural parameters taken into consideration.[9] Although usually underrated, the computational conformation analysis of flexible molecules is the most important step of whole analysis and should be done with the highest available accuracy.[10]

Since there is no possibility to directly confront the conformational equilibria of **1**-**10** with the experiment, the choice of the best method of geometry/energy determination can be done indirectly either by comparising the calculated ECD with the experimental data, or by invoking literature precedents. The last "copy-paste" approach however may fail if one takes everything at face value. Since the compounds investigated, contain naphthalene moieties it is expected that they may have an effect on each other, and by this determine the overall conformation of molecule. Due to the size of the compounds studied, the recommended approach for estimation of the eventuality of π/π interaction by the use of *ab initio* coupled cluster calculations with single and double substitutions with noniterative triple excitations [CCSD(T)] together with enhanced basis set (preferably augmented-valence triple-ξ with polarisation functions) is rather unrealistic vision. On the other hand the cheaper and computationally simpler alternative like as second-order Møller-Plesset perturbation theory is widely used,[11] although it is also known that the MP2 method tends to overestimate this contribution.

In our studies we used approach that includes (i) systematic conformational search at molecular mechanics level, (ii) pre-optimization of energy minima at the PBE0/6-31G(d) level, that reduce number of possible structures, (iii) re-optimization of conformers found at low-DFT level at DFT/6-311++G(d,p) level followed by frequency calculation, that confirmed stability of calculated structures, (iv) single-point energy calculations at the MP2/6-311++G(d,p) level (v) calculations on relative energies (ΔE_{DFT}, ΔG_{DFT} and ΔE_{MP2}) using Boltzmann statistics and T = 298.15 K (vi) calculations of rotatory strengths at the TD-DFT/6-311++G(d,p) level for all stable conformers ranging from 0.0 to 2.0 kcal mol^{-1} in relative energies.

Preliminary conformer distribution search was performed by the Scigress package[12] using the MM3 molecular mechanics force field. The systematic search of all possible conformers has been performed using molecular mechanics method taking into account the degrees of freedom of the molecule. The real minimum energy conformers found by molecular mechanics were further fully optimized at the PBE0/6-31G(d) level as implemented in the Gaussian09 package.[13] This reduced significantly the number of conformers. For higher accuracy calculations we used four different functionals including pure functional with empirical dispersion correction B97-D[14], hybrid functional PBE0[15] and long-range corrected modification of PBE, called LC-wPBE[16] and newly developed by Thruhlar and coworkers M06-2X functional.[17] All calculations with the use of DFT methods started from structures obtained from molecular mechanics and pre-optimized at PBE0/6-31G(d) level. Then all stable conformers, regardless their relative energies, were re-optimized at the DFT/6-311++G(d,p) or DFT/6-311G(2d,p) levels, using the same density functionals as for preliminary optimization. These conformers were the real minima (no imaginary frequencies have been found). Additionally the single-point energies were calculated at the B2PLYP-D/6-311++G(d,p) and MP2/6-311++G(d,p) level for all stable conformers.

Total and free energy values have been calculated and used to obtain the Boltzmann population of conformers at 298.15 K. Only the results for conformers that differ from the most stable one by less than 2 kcal mol^{-1} have been taken into account for further calculations, following a generally accepted protocol.[18]

The TD-DFT/6-311++G(d,p) calculations of ECD of **1a**, **5a**-**6a**, **10a**-**15** were performed for all structures re-optimized at higher levels of theory. We used five different density functionals for calculation of rotatory strengths: PBE0[15], LC-wPBE,[16] CAM-B3LYP,[19] hybrid part of B2PLYP functional[20] and M06-2X functional.[17] Rotatory strengths were calculated using both length and velocity representations. In the present study, the differences between the length and velocity representations of the calculated values of rotatory strengths were quite small, and for this reason only the velocity representations were further used. The CD spectra were simulated by overlapping Gaussian functions for each transition according to the procedure previously described.[21] Since the all ECD measurements were done in non-polar environment, the solvent dielectric constant was not taken into account during calculations.

Note that in figures presented in Supporting Info, rotatory strengths calculated using velocity representations were Gaussian-fitted with the use of 0.3 eV the exponential half-widths at 1/e height whereas rotatory strengths calculated using length representations were Gaussian-fitted with the use of 0.4 eV the exponential half-widths at 1/e height.

A good agreement between the calculated and the experimental UV/CD spectra was observed regardless the method used for structure/spectra calculations, however the best results in term of consistency were obtained using the LC-wPBEO/6-311++G(d,p) method for structure refining and ΔG-based conformer distributions and TD-B2LYP/6-311++G(2d,2p) method for calculations of CD spectra.

We did not observe any advantage of MP2 and B2PLYP-D methods for calculations of energies and conformers distributions. In general these methods overestimate the role of π-π interactions between naphthalene rings, thus, the conformers in which these interactions were possible were characterized by the lowest values of relative energies. In some cases this situation affected calculated Boltzmann-averaged ECD spectra. To sum-up, in the case of dinapthyl esters the use of balanced long-range corrected hybrid functional provided better and more consistent results that use of MP2 method or dispersion-corrected functionals.

References

1. C. R. Groom, I. J. Bruno, M. P. Lightfoot and S. C. Ward, *Acta Cryst.* **2016**, *B72*, 171.
2. CrysAlisPRO, Agilent Technologies, Yarnton, Oxfordshire, England, 2014.
3. Sheldrick, G. M. *Acta Cryst.* **2008**, *A*64, 112.
4. Sheldrick, G. M. *Acta Cryst*. **2015**, *C*71, 3.
5. H. D. Flack, *Acta Cryst.* **1983**, A39, 876.
6. Bruno, I. J.; Cole, J. C.; Edgington, P. R.; Kessler, M.; Macrae, C. F.; McCabe, P.; Pearson, J.; Taylor, R.; *Acta Cryst*., **2002**, *B*58, 389.
7. (a) Mori, T.; Inoue, Y.; Grimme, S. *J. Org. Chem.* **2006**, *71*, 9797; (b) Marchesan, D.; Coriani, S.; Forzato, C.; Nitti, P.; Pitacco, G.; Ruud, K. *J. Phys. Chem. A* **2005**, *109*, 1449; (c) Grimme, S.; Bahlmann, A.; Haufe, G. *Chirality* **2002**, *14*, 793; (d) Kwit, M.; Sharma, N. D.; Boyd, D. R.; Gawronski, J. *Chirality* **2008**, *20*, 609; (e) Kwit, M.; Sharma, N. D.; Boyd, D. R.; Gawronski, J. *Chem. Eur. J.* **2007**, *13*, 5812.
8. (a) Pecul, M. *Chem. Phys. Lett.* **2006**, *418*, 1; (b) Kundrat, M. D.; Autschbach, J. *J. Phys. Chem. A* **2006**, *110*, 4115; (c) Kundrat, M. D.; Autschbach, J. *J. Phys. Chem. A* **2006**, *110*, 12908; (d) Pecul, M.; Ruud, K.; Rizzo, A.; Helgaker, T. *J. Phys. Chem. A* **2004**, *108*, 4269; (e) Wiberg, K. B.; Vaccaro, P. H.; Cheeseman, J. R. *J. Am. Chem. Soc.* **2003**, *125*, 1888; (f) Specht, K. M.; Nam, J.; Ho, D. M.; Berova, N.; Kondru, R. K.; Beratan, D. N.; Wipf, P.; Pascal, R. A. Jr.; Kahne, D. *J. Am. Chem. Soc.* **2001**, *123*, 8961;
9. (a) Cramer, C. J. *Essentials of Computational Chemistry*; Wiley: Chichester, 2004. (b) Young, D. C. *Computational Chemistry*; Wiley-Interscience: New York, 2001.
10. Kwit, M.; Rozwadowska, M. D.; Gawroński, J.; Grajewska, A. *J. Org. Chem.* **2009**, *74*, 8051-8063.
11. See for example: (a) C. Gonzalez, E. C. Lim, *J. Phys. Chem. A* **2000**, *104*, 2953; (b) M. Saeki, H. Akagi, M. Fujii, *J. Chem. Theory Comput*. **2006**, *2*, 1176; (c) T.R. Walsh, *Chem. Phys. Lett*. **2002**, *363*, 45.
12. Scigress 2.5, Fujitsu Ltd.
13. Gaussian 09, Revision A.1, M. J. Frisch, G. W. Trucks, H. B. Schlegel, G. E. Scuseria, M. A. Robb, J. R. Cheeseman, G. Scalmani, V. Barone, B. Mennucci, G. A. Petersson, H. Nakatsuji, M. Caricato, X. Li, H. P. Hratchian, A. F. Izmaylov, J. Bloino, G. Zheng, J. L. Sonnenberg, M. Hada, M. Ehara, K. Toyota, R. Fukuda, J. Hasegawa, M. Ishida, T. Nakajima, Y. Honda, O. Kitao, H. Nakai, T. Vreven, J. A. Montgomery, Jr., J. E. Peralta, F. Ogliaro, M. Bearpark, J. J. Heyd, E. Brothers, K. N. Kudin, V. N. Staroverov, R. Kobayashi, J. Normand, K. Raghavachari, A. Rendell, J. C. Burant, S. S. Iyengar, J. Tomasi, M. Cossi, N. Rega, J. M. Millam, M. Klene, J. E. Knox, J. B. Cross, V. Bakken, C. Adamo, J. Jaramillo, R. Gomperts, R. E. Stratmann, O. Yazyev, A. J. Austin, R. Cammi, C. Pomelli, J. W. Ochterski, R. L. Martin, K. Morokuma, V. G. Zakrzewski, G. A. Voth, P. Salvador, J. J. Dannenberg, S. Dapprich, A. D. Daniels, Ö. Farkas, J. B. Foresman, J. V. Ortiz, J. Cioslowski, and D. J. Fox, Gaussian, Inc., Wallingford CT, 2009.
14. P. J. Stephens, F. J. Devlin, J. R. Cheeseman, M. J. Frisch, O. Bortolini, P. Besse, *Chirality* **2003**, *15*, S57.
15. S. Grimme, *J. Comp. Chem.* **2006**, *27*, 1787.
16. C. Adamo, V. Barone, *J. Chem. Phys.* **1999**, *110*, 6158.
17. a) O. A. Vydrov, G. E. Scuseria, *J. Chem. Phys.* **2006**, *125*, 234109; b) O. A. Vydrov, J. Heyd, A. Krukau, G. E. Scuseria, *J. Chem. Phys.* **2006**, *125*, 074106; c) O. A. Vydrov, G. E. Scuseria, J. P. Perdew, *J. Chem. Phys.* **2007**, *126*, 154109.
18. T. Yanai, D. Tew, N. Handy, *Chem. Phys. Lett.* **2004**, *393*, 51.
19. Y. Zhao, D. G. Truhlar, *Theor. Chem. Acc.* **2008**, *120*, 215.

20. a) S. Grimme, *J. Chem. Phys.* **2006**, *124*, 034108; b) T. Schwabe, S. Grimme, *Phys. Chem. Chem. Phys.* **2007**, *9*, 3397.
21. N. Harada, P. J. Stephens, *Chirality* **2010**, *22*, 229-233;

Table SA1. Total energies (E_{DFT}, in Hartree), relative energies (ΔE_{DFT}, ΔG_{DFT}, $\Delta E_{B2PLYP-D}$, ΔE_{MP2}, in kcal mol^{-1}) and percentage populations of low-energy conformers of **1a** calculated at B2PLYP-D/6-311++G(d,p)//B97-D/6-311++G(d,p) and MP2/6-311++G(d,p)//B97-D/6-311++G(d,p) levels.

Conf.[a]	E_{DFT}	ΔE_{DFT}	Pop.	ΔG_{DFT}	Pop.	$\Delta E_{B2PLYP-D}$	Pop.	E_{MP2}	Pop.
2	-1265.082103	0.00	96	0.00	79	0.00	96	0.00	100
16	-1265.078702	2.13		1.58	6	2.15		4.09	
23	-1265.078992	1.95	4	1.15	11	1.86	4	3.12	
35	-1265.074285	4.91		1.84	4	6.07		11.54	

[a] Conformers are numbered in the order of appearance in the conformational search.

Table SA2. Total energies (E_{DFT}, in Hartree), relative energies (ΔE_{DFT}, ΔG_{DFT}, $\Delta E_{B2PLYP-D}$, ΔE_{MP2}, in kcal mol^{-1}) and percentage populations of low-energy conformers of **1a** calculated at B2PLYP-D/6-311++G(d,p)//PBE0/6-311++G(d,p) and MP2/6-311++G(d,p)//PBE0/6-311++G(d,p) levels.

Conf.[a]	E_{DFT}	ΔE_{DFT}	Pop.	ΔG_{DFT}	Pop.	ΔE_{B2PLYP}	Pop.	ΔE_{MP2}	Pop.
2	-1264.51097	0.00	57	0.78	6	0	96	0	85
3	-1264.50646	2.83		1.76	1	3.42		3.79	
16	-1264.50787	1.95	2	1.39	2	1.91	4	1.26	10
19	-1264.50753	2.16		1.20	3	6.17		9.24	
23	-1264.5078	1.99	2	1.29	3	2.21		1.73	5
24	-1264.50565	3.34		1.47	2	6.00		8.05	
25	-1264.50998	0.62	20	0.00	24	2.69		4.19	
26	-1264.50964	0.83	14	0.15	18	2.53		3.74	
28	-1264.50871	1.42	5	0.06	22	4.26		6	
29	-1264.50692	2.54		1.52	2	5.26		6.9	
31	-1264.50673	2.66		1.26	3	5.27		6.81	
32	-1264.50727	2.33		0.71	7	5.98		8.63	
33	-1264.50763	2.10		0.71	7	6.03		8.86	

[a] Conformers are numbered in the order of appearance in the conformational search.

Table SA3. Total energies (E_{DFT}, in Hartree), relative energies (ΔE_{DFT}, ΔG_{DFT}, $\Delta E_{B2PLYP-D}$, ΔE_{MP2}, in kcal mol^{-1}) and percentage populations of low-energy conformers of **1a** calculated at B2PLYP-D/6-311++G(d,p)//LC-wPBE/6-311++G(d,p) and MP2/6-311++G(d,p)//LC-wPBE/6-311++G(d,p) levels.

Conf.[a]	E_{DFT}	ΔE_{DFT}	Pop.	ΔG_{DFT}	Pop.	ΔE_{B2PLYP}	Pop.	ΔE_{MP2}	Pop.
2	-1265.06708	0.00	63	1.54	4	0.00	91	0.00	75
16	-1265.063976	1.95	2	2.45		1.65	6	0.88	17
17	-1265.063036	2.54		1.25	6	5.93		8.57	
23	-1265.063857	2.02		2.44		1.95	3	1.35	8
25	-1265.065869	0.76	17	0.68	15	2.6		3.95	
26	-1265.065636	0.91	14	0.77	13	2.48		3.59	
28	-1265.064528	1.60	4	0.00	48	4.12		5.62	
32	-1265.062911	2.62		1.62	3	5.67		8.04	
33	-1265.063062	2.52		1.34	5	5.86		8.45	

[a] Conformers are numbered in the order of appearance in the conformational search.

Table SA4. Total energies (E_{DFT}, in Hartree), relative energies (ΔE_{DFT}, ΔG_{DFT}, $\Delta E_{B2PLYP-D}$, ΔE_{MP2}, in kcal mol^{-1}) and percentage populations of low-energy conformers of **1a** calculated at B2PLYP-D/6-311++G(d,p)//M06-2X/6-311++G(d,p) and MP2/6-311++G(d,p)//M06-2X/6-311++G(d,p) levels.

Conf.[a]	E_{DFT}	ΔE_{DFT}	Pop.	ΔG_{DFT}	Pop.	ΔE_{B2PLYP}	Pop.	ΔE_{MP2}	Pop.
2	-1265.479	0.00	95	0.00	62	0.00	97	0.00	100
16	-1265.475903	1.69	5	1.12	9	1.99	3	2.49	
23	-1265.475383	2.02		1.03	11	2.12		2.9	
25	-1265.474201	2.76		1.16	9	3.32		5.66	
26	-1265.474365	2.66		1.12	9	3.26		5.54	

[a] Conformers are numbered in the order of appearance in the conformational search.

Table SB1. Total energies (E_{DFT}, in Hartree), relative energies (ΔE_{DFT}, ΔG_{DFT}, $\Delta E_{B2PLYP-D}$, ΔE_{MP2}, in kcal mol^{-1}) and percentage populations of low-energy conformers of **2a** calculated at B2PLYP-D/6-311++G(d,p)//B97-D/6-311++G(d,p) and MP2/6-311++G(d,p)//B97-D/6-311++G(d,p) levels.

Conf.[a]	E_{DFT}	ΔE_{DFT}	Pop.	ΔG_{DFT}	Pop.	$\Delta E_{B2PLYP-D}$	Pop.	E_{MP2}	Pop.
2	-1376.176035	0.33	31	0.00	93	0.42	29	0.46	28
3	-1376.176563	0.00	54	1.96	3	0.00	60	0.00	60
4	-1376.175331	0.77	15	1.94	4	1.02	11	0.94	12

[a] Conformers are numbered in the order of appearance in the conformational search.

Table SB2. Total energies (E_{DFT}, in Hartree), relative energies (ΔE_{DFT}, ΔG_{DFT}, $\Delta E_{B2PLYP-D}$, ΔE_{MP2}, in kcal mol^{-1}) and percentage populations of low-energy conformers of **2a** calculated at B2PLYP-D/6-311++G(d,p)//PBE0/6-311++G(d,p) and MP2/6-311++G(d,p)//PBE0/6-311++G(d,p) levels.

Conf.[a]	E_{DFT}	ΔE_{DFT}	Pop.	ΔG_{DFT}	Pop.	$\Delta E_{B2PLYP-D}$	Pop.	E_{MP2}	Pop.
1	-1375.56886	0.00	63	1.91	4	0.00	66	0.00	58
2	-1375.56806	0.50	27	0.00	96	1.08	11	0.86	14
3	-1375.56677	1.31	67	2.87		0.69	20	0.50	25
4	-1375.56604	1.77	3	2.76		1.83	3	1.78	3

[a] Conformers are numbered in the order of appearance in the conformational search.

Table SB3. Total energies (E_{DFT}, in Hartree), relative energies (ΔE_{DFT}, ΔG_{DFT}, $\Delta E_{B2PLYP-D}$, ΔE_{MP2}, in kcal mol^{-1}) and percentage populations of low-energy conformers of **5a** calculated at B2PLYP-D/6-311++G(d,p)//LC-wPBE/6-311++G(d,p) and MP2/6-311++G(d,p)//LC-wPBE/6-311++G(d,p) levels.

Conf.[a]	E_{DFT}	ΔE_{DFT}	Pop.	ΔG_{DFT}	Pop.	$\Delta E_{B2PLYP-D}$	Pop.	E_{MP2}	Pop.
1	-1376.16557	0.00	62	0.80	18	0	66	0.00	67
2	-1376.164768	0.50	27	0.00	69	1.03	12	1.00	12
3	-1376.163617	1.23	8	1.57	5	0.75	19	0.78	18
4	-1376.162819	1.73	3	1.25	8	1.81	3	1.83	3

[a] Conformers are numbered in the order of appearance in the conformational search.

Table SB4. Total energies (E_{DFT}, in Hartree), relative energies (ΔE_{DFT}, ΔG_{DFT}, $\Delta E_{B2PLYP-D}$, ΔE_{MP2}, in kcal mol^{-1}) and percentage populations of low-energy conformers of **5a** calculated at B2PLYP-D/6-311++G(d,p)//M06-2X/6-311++G(d,p) and MP2/6-311++G(d,p)//M06-2X/6-311++G(d,p) levels.

Conf.[a]	E_{DFT}	ΔE_{DFT}	Pop.	ΔG_{DFT}	Pop.	$\Delta E_{B2PLYP-D}$	Pop.	E_{MP2}	Pop.
1	-1376.608433	0.00	78	1.37	9	0.00	67	0.00	57
2	-1376.606756	1.05	13	0.00	91	1.06	11	0.75	16
3	-1376.60642	1.26	9	2.33		0.74	19	0.53	23
4	-1376.604836	2.26		2.02		1.84	3	1.56	4

[a] Conformers are numbered in the order of appearance in the conformational search.

Table SC1. Total energies (E_{DFT}, in Hartree), relative energies (ΔE_{DFT}, ΔG_{DFT}, $\Delta E_{B2PLYP-D}$, ΔE_{MP2}, in kcal mol^{-1}) and percentage populations of low-energy conformers of **6a** calculated at B2PLYP-D/6-311++G(d,p)//B97-D/6-311++G(d,p) and MP2/6-311++G(d,p)//B97-D/6-311++G(d,p) levels.

Conf.[a]	E_{DFT}	ΔE_{DFT}	Pop.	ΔG_{DFT}	Pop.	$\Delta E_{B2PLYP-D}$	Pop.	E_{MP2}	Pop.
4	-1263.835506	0.86	15	1.21	5	1.67	5	4.44	
5	-1263.834955	1.21	9	1.77	2	2.19		5.09	
13	-1263.835106	1.11	10	1.53	3	1.71	5	3.17	
14	-1263.83688	0.00	66	1.63	3	0.00	90	0.00	100
18	-1263.833454	2.15		1.26	5	4.27		9.89	
22	-1263.833552	2.09		0.00	40	2.65		8.13	
23	-1263.833249	2.28		1.71	2	2.84		7.56	
24	-1263.833552	2.09		0.09	35	2.65		8.13	
26	-1263.832478	2.76		1.60	3	3.49		9.04	
36	-1263.832198	2.94		1.72	2	3.19		4.44	

[a] Conformers are numbered in the order of appearance in the conformational search.

Table SC2. Total energies (E_{DFT}, in Hartree), relative energies (ΔE_{DFT}, ΔG_{DFT}, $\Delta E_{B2PLYP-D}$, ΔE_{MP2}, in kcal mol^{-1}) and percentage populations of low-energy conformers of **6a** calculated at B2PLYP-D/6-311++G(d,p)//PBE0/6-311++G(d,p) and MP2/6-311++G(d,p)//PBE0/6-311++G(d,p) levels.

Conf.[a]	E_{DFT}	ΔE_{DFT}	Pop.	ΔG_{DFT}	Pop.	$\Delta E_{B2PLYP-D}$	Pop.	E_{MP2}	Pop.
18	-1263.278787	0.00	34	1.03	9	0	31	0.00	32
22	-1263.278624	0.10	29	0.00	46	0.12	26	0.03	32
23	-1263.276630	1.35	3	1.56	3	0.6	11	1.10	5
24	-1263.278599	0.12	28	0.13	37	0.26	20	0.15	25
26	-1263.276386	1.51	3	1.75	2	1.07	6	1.41	3
36	-1263.276602	1.37	3	1.55	3	1.01	6	1.24	4

[a] Conformers are numbered in the order of appearance in the conformational search.

Table SC3. Total energies (E_{DFT}, in Hartree), relative energies (ΔE_{DFT}, ΔG_{DFT}, $\Delta E_{B2PLYP-D}$, ΔE_{MP2}, in kcal mol^{-1}) and percentage populations of low-energy conformers of **6a** calculated at B2PLYP-D/6-311++G(d,p)//LC-wPBE/6-311++G(d,p) and MP2/6-311++G(d,p)//LC-wPBE/6-311++G(d,p) levels.

Conf.[a]	E_{DFT}	ΔE_{DFT}	Pop.	ΔG_{DFT}	Pop.	$\Delta E_{B2PLYP-D}$	Pop.	E_{MP2}	Pop.
18	-1263.824339	0.00	31	0.50	16	0.06	24	0.46	15
22	-1263.824296	0.03	28	0.01	37	0	27	0.25	22
23	-1263.822596	1.09	5	1.71	3	0.3	16	0.00	34
24	-1263.824242	0.06	28	0.00	37	0.28	17	0.77	9
26	-1263.822453	1.18	4	1.42	3	0.61	10	0.51	14
36	-1263.822468	1.17	4	1.27	4	0.85	6	0.98	6

[a] Conformers are numbered in the order of appearance in the conformational search.

Table SC4. Total energies (E_{DFT}, in Hartree), relative energies (ΔE_{DFT}, ΔG_{DFT}, $\Delta E_{B2PLYP-D}$, ΔE_{MP2}, in kcal mol^{-1}) and percentage populations of low-energy conformers of **6a** calculated at B2PLYP-D/6-311++G(d,p)//M06-2X/6-311++G(d,p) and MP2/6-311++G(d,p)//M06-2X/6-311++G(d,p) levels.

Conf.[a]	E_{DFT}	ΔE_{DFT}	Pop.	ΔG_{DFT}	Pop.	$\Delta E_{B2PLYP-D}$	Pop.	E_{MP2}	Pop.
3	-1264.241837	0.40	12	3.29		0.00	34	0.00	100
4	-1264.241571	0.57	9	3.20		0.29	21	3.3	
5	-1264.240234	1.40	2	3.63		1.14	5	3.97	
14	-1264.242472	0.00	24	2.44		0.12	28	2.32	
18	-1264.24173	0.47	11	1.04	7	1.6	2	8.1	
22	-1264.241641	0.52	9	0.00	42	1.95	1	8.76	
23	-1264.240152	1.46	2	1.27	5	2.44		8.77	
24	-1264.24154	0.58	9	0.23	29	2.04		8.88	
26	-1264.239909	1.61	2	1.27	5	2.96		9.68	
36	-1264.24008	1.50	2	1.42	4	2.69		9.21	
39	-1264.242177	0.19	18	0.99	8	0.77	9	6.11	

[a] Conformers are numbered in the order of appearance in the conformational search.

Table SD1. Total energies (E_{DFT}, in Hartree), relative energies (ΔE_{DFT}, ΔG_{DFT}, $\Delta E_{B2PLYP-D}$, ΔE_{MP2}, in kcal mol^{-1}) and percentage populations of low-energy conformers of **7a** calculated at B2PLYP-D/6-311++G(d,p)//B97-D/6-311++G(d,p) and MP2/6-311++G(d,p)//B97-D/6-311++G(d,p) levels.

Conf.[a]	E_{DFT}	ΔE_{DFT}	Pop.	ΔG_{DFT}	Pop.	$\Delta E_{B2PLYP-D}$	Pop.	E_{MP2}	Pop.
7	-1303.132877	0.00	62	1.18	12	0.00	67	0.00	100
32	-1303.132403	0.30	38	0.00	85	0.43	33	2.20	
35	-1303.126564	3.96		1.95	3	5.02		9.79	

[a] Conformers are numbered in the order of appearance in the conformational search.

Table SD2. Total energies (E_{DFT}, in Hartree), relative energies (ΔE_{DFT}, ΔG_{DFT}, $\Delta E_{B2PLYP-D}$, ΔE_{MP2}, in kcal mol^{-1}) and percentage populations of low-energy conformers of **7a** calculated at B2PLYP-D/6-311++G(d,p)//PBE0/6-311++G(d,p) and MP2/6-311++G(d,p)//PBE0/6-311++G(d,p) levels.

Conf.[a]	E_{DFT}	ΔE_{DFT}	Pop.	ΔG_{DFT}	Pop.	$\Delta E_{B2PLYP-D}$	Pop.	E_{MP2}	Pop.
3	-1302.551765	0.59	10	1.43	4	3.49		0.24	12
7	-1302.551607	0.69	8	0.28	26	3.23		0.06	16
8	-1302.551687	0.64	9	0.00	41	3.34		0.09	15
18	-1302.551721	0.62	9	1.62	3	3.02		0.52	7
26	-1302.551609	0.69	8	1.04	7	3.17		0.00	17
32	-1302.552084	0.39	14	0.91	9	1.16	12	1.05	3
35	-1302.551601	0.69	8	1.30	4	3.52		0.24	12
39	-1302.552707	0.00	26	1.67	2	0.00	88	0.46	8
61	-1302.551553	0.72	8	1.34	4	3.63		0.28	11

[a] Conformers are numbered in the order of appearance in the conformational search.

Table SD3. Total energies (E_{DFT}, in Hartree), relative energies (ΔE_{DFT}, ΔG_{DFT}, $\Delta E_{B2PLYP-D}$, ΔE_{MP2}, in kcal mol^{-1}) and percentage populations of low-energy conformers of **7a** calculated at B2PLYP-D/6-311++G(d,p)//LC-wPBE/6-311++G(d,p) and MP2/6-311++G(d,p)//LC-wPBE/6-311++G(d,p) levels.

Conf.[a]	E_{DFT}	ΔE_{DFT}	Pop.	ΔG_{DFT}	Pop.	$\Delta E_{B2PLYP-D}$	Pop.	E_{MP2}	Pop.
3	-1303.123112	0.72	8	0.00	46	3.51		5.79	
7	-1303.123219	0.65	9	0.83	11	3.12		4.94	
8	-1303.123257	0.63	9	1.03	8	3.14		5.08	
14	-1303.123367	0.56	11	1.05	8	2.9		4.48	
18	-1303.123095	0.73	8	1.76	2	3.07		4.93	
25	-1303.124254	0.00	28	1.92	2	0.00	89	0.00	100
26	-1303.123255	0.63	9	0.83	11	3.18		5.08	
32	-1303.123372	0.55	11	1.14	7	1.22	11	2.01	
35	-1303.122992	0.79	7	1.32	5	3.53		5.78	

[a] Conformers are numbered in the order of appearance in the conformational search.

Table SD4. Total energies (E_{DFT}, in Hartree), relative energies (ΔE_{DFT}, ΔG_{DFT}, $\Delta E_{B2PLYP-D}$, ΔE_{MP2}, in kcal mol^{-1}) and percentage populations of low-energy conformers of **7a** calculated at B2PLYP-D/6-311++G(d,p)//M06-2X/6-311++G(d,p) and MP2/6-311++G(d,p)//M06-2X/6-311++G(d,p) levels.

Conf.[a]	E_{DFT}	ΔE_{DFT}	Pop.	ΔG_{DFT}	Pop.	$\Delta E_{B2PLYP-D}$	Pop.	E_{MP2}	Pop.
3	-1303.54038	1.40	6	0.13	25	2.51		6.3	
7	-1303.54072	1.19	8	0.25	21	1.77	5	4.82	
18	-1303.54088	1.09	10	0.00	30	2.09		5.45	
26	-1303.54059	1.27	7	0.54	13	2	3	5.19	
35	-1303.54054	1.30	7	1.29	4	2.57		6.51	
61	-1303.54261	0.00	62	1.41	3	0.00	92	0.00	100
73	-1303.53799	2.90		1.26	4	3.32		5.75	

[a] Conformers are numbered in the order of appearance in the conformational search.

Table SE1. Total energies (E_{DFT}, in Hartree), relative energies (ΔE_{DFT}, ΔG_{DFT}, $\Delta E_{B2PLYP-D}$, ΔE_{MP2}, in kcal mol^{-1}) and percentage populations of low-energy conformers of **8a** calculated at B2PLYP-D/6-311++G(d,p)//B97-D/6-311++G(d,p) and MP2/6-311++G(d,p)//B97-D/6-311++G(d,p) levels.

Conf.[a]	E_{DFT}	ΔE_{DFT}	Pop.	ΔG_{DFT}	Pop.	$\Delta E_{B2PLYP-D}$	Pop.	E_{MP2}	Pop.
2	-1342.461159	0.00	100	0.00	52	0.00	100	0.00	100
4	-1342.453	4.90		1.28	6	5.97		11.58	
6	-1342.453812	4.61		1.39	5	5.74		9.67	
11	-1342.454162	4.39		1.30	6	5.15		10.4	
12	-1342.455173	3.76		0.52	22	4.74		9.51	
16	-1342.453	5.30		1.68	3	6.52		11.33	
24	-1342.45303	5.10		1.32	6	6.13		11.47	

[a] Conformers are numbered in the order of appearance in the conformational search.

Table SE2. Total energies (E_{DFT}, in Hartree), relative energies (ΔE_{DFT}, ΔG_{DFT}, $\Delta E_{B2PLYP-D}$, ΔE_{MP2}, in kcal mol^{-1}) and percentage populations of low-energy conformers of **8a** calculated at B2PLYP-D/6-311++G(d,p)//PBE0/6-311++G(d,p) and MP2/6-311++G(d,p)//PBE0/6-311++G(d,p) levels.

Conf.[a]	E_{DFT}	ΔE_{DFT}	Pop.	ΔG_{DFT}	Pop.	$\Delta E_{B2PLYP-D}$	Pop.	E_{MP2}	Pop.
2	-1341.855408	0.62	14	1.42	5	0.00	53	2.20	
4	-1341.856392	0.00	41	0.00	58	1.61	3	0.00	54
6	-1341.855034	0.85	9	0.84	14	2.38		1.47	5
11	-1341.855301	0.68	13	1.85	2	0.36	28	1.10	9
12	-1341.855596	0.50	17	0.85	13	0.96	10	0.69	16
16	-1341.853475	1.83	2	1.75	3	2.32		1.62	3
24	-1341.854333	1.29	4	1.41	5	1.38	6	0.81	13

[a] Conformers are numbered in the order of appearance in the conformational search.

Table SE3. Total energies (E_{DFT}, in Hartree), relative energies (ΔE_{DFT}, ΔG_{DFT}, $\Delta E_{B2PLYP-D}$, ΔE_{MP2}, in kcal mol^{-1}) and percentage populations of low-energy conformers of **8a** calculated at B2PLYP-D/6-311++G(d,p)//LC-wPBE/6-311++G(d,p) and MP2/6-311++G(d,p)//LC-wPBE/6-311++G(d,p) levels.

Conf.[a]	E_{DFT}	ΔE_{DFT}	Pop.	ΔG_{DFT}	Pop.	$\Delta E_{B2PLYP-D}$	Pop.	E_{MP2}	Pop.
2	-1342.453544	0.00	36	0.26	22	0.51	17	0.70	11
4	-1342.453051	0.31	22	0.00	35	1.52	3	2.55	
6	-1342.452811	0.46	17	0.05	33	2.22		3.81	
11	-1342.452066	0.93	8	2.13		0.19	29	0.39	18
12	-1342.452646	0.56	14	1.77	2	0.00	38	0	35
14	-1342.447394	3.86		5.46		1.03	7	0.11	30
24	-1342.451259	1.43	3	1.29	4	1.13	6	1.05	6
27	-1342.449541	2.51		1.06	6	3.14		4.17	

[a] Conformers are numbered in the order of appearance in the conformational search.

Table SE4. Total energies (E_{DFT}, in Hartree), relative energies (ΔE_{DFT}, ΔG_{DFT}, $\Delta E_{B2PLYP-D}$, ΔE_{MP2}, in kcal mol^{-1}) and percentage populations of low-energy conformers of **8a** calculated at B2PLYP-D/6-311++G(d,p)//M06-2X/6-311++G(d,p) and MP2/6-311++G(d,p)//M06-2X/6-311++G(d,p) levels.

Conf.[a]	E_{DFT}	ΔE_{DFT}	Pop.	ΔG_{DFT}	Pop.	$\Delta E_{B2PLYP-D}$	Pop.	E_{MP2}	Pop.
2	-1342.88778	0.00	100	0.00	100	0.00	100	0.00	100

[a] Conformers are numbered in the order of appearance in the conformational search.

Table SF1. Total energies (E_{DFT}, in Hartree), relative energies (ΔE_{DFT}, ΔG_{DFT}, $\Delta E_{B2PLYP-D}$, ΔE_{MP2}, in kcal mol^{-1}) and percentage populations of low-energy conformers of **9a** calculated at B2PLYP-D/6-311++G(d,p)//B97-D/6-311++G(d,p) and MP2/6-311++G(d,p)//B97-D/6-311++G(d,p) levels.

Conf.[a]	E_{DFT}	ΔE_{DFT}	Pop.	ΔG_{DFT}	Pop.	$\Delta E_{B2PLYP-D}$	Pop.	E_{MP2}	Pop.
3	-1381.759341	0.82	20	0.63	24	1.51	7	3.5	
10	-1381.75665	2.50		1.58	5	2.95		4.74	
19	-1381.761	0.00	80	0.00	71	0.00	98	0.00	100

[a] Conformers are numbered in the order of appearance in the conformational search.

Table SF2. Total energies (E_{DFT}, in Hartree), relative energies (ΔE_{DFT}, ΔG_{DFT}, $\Delta E_{B2PLYP-D}$, ΔE_{MP2}, in kcal mol^{-1}) and percentage populations of low-energy conformers of **9a** calculated at B2PLYP-D/6-311++G(d,p)//PBE0/6-311++G(d,p) and MP2/6-311++G(d,p)//PBE0/6-311++G(d,p) levels.

Conf.[a]	E_{DFT}	ΔE_{DFT}	Pop.	ΔG_{DFT}	Pop.	$\Delta E_{B2PLYP-D}$	Pop.	E_{MP2}	Pop.
2	-1381.14084542	0.00	76	0.78	20	0.00	94	0.00	70
11	-1381.13963676	0.76	21	0.00	74	2.19		2.43	
19	-1381.13779889	1.91	3	1.46	6	1.63	6	0.49	30

[a] Conformers are numbered in the order of appearance in the conformational search.

Table SF3. Total energies (E_{DFT}, in Hartree), relative energies (ΔE_{DFT}, ΔG_{DFT}, $\Delta E_{B2PLYP-D}$, ΔE_{MP2}, in kcal mol^{-1}) and percentage populations of low-energy conformers of **9a** calculated at B2PLYP-D/6-311++G(d,p)//LC-wPBE/6-311++G(d,p) and MP2/6-311++G(d,p)//LC-wPBE/6-311++G(d,p) levels.

Conf.[a]	E_{DFT}	ΔE_{DFT}	Pop.	ΔG_{DFT}	Pop.	$\Delta E_{B2PLYP-D}$	Pop.	E_{MP2}	Pop.
2	-1381.763378	0.00	79	1.29	10	0.00	95	0.00	81
11	-1381.762104	0.80	21	0.00	86	2.21		3.01	
19	-1381.76018	2.01		1.73	4	1.72	5	0.88	19

[a] Conformers are numbered in the order of appearance in the conformational search.

Table SF4. Total energies (E_{DFT}, in Hartree), relative energies (ΔE_{DFT}, ΔG_{DFT}, $\Delta E_{B2PLYP-D}$, ΔE_{MP2}, in kcal mol^{-1}) and percentage populations of low-energy conformers of **9a** calculated at B2PLYP-D/6-311++G(d,p)//M06-2X/6-311++G(d,p) and MP2/6-311++G(d,p)//M06-2X/6-311++G(d,p) levels

Conf.[a]	E_{DFT}	ΔE_{DFT}	Pop.	ΔG_{DFT}	Pop.	$\Delta E_{B2PLYP-D}$	Pop.	E_{MP2}	Pop.
3	-1382.193625	0.74	22	0.44	30	1.55	7	4.24	
10	-1382.190756	2.54		1.35	6	2.84		5.66	
19	-1382.19481	0.00	78	0.00	64	0.00	93	0.00	100

[a] Conformers are numbered in the order of appearance in the conformational search.

Table SG1. Total energies (E_{DFT}, in Hartree), relative energies (ΔE_{DFT}, ΔG_{DFT}, $\Delta E_{B2PLYP-D}$, ΔE_{MP2}, in kcal mol^{-1}) and percentage populations of low-energy conformers of **10a** calculated at B2PLYP-D/6-311++G(d,p)//B97-D/6-311++G(d,p) and MP2/6-311++G(d,p)//B97-D/6-311++G(d,p) levels

Conf.[a]	E_{DFT}	ΔE_{DFT}	Pop.	ΔG_{DFT}	Pop.	$\Delta E_{B2PLYP-D}$	Pop.	E_{MP2}	Pop.
1	-1380.531372	0.00	100	0.00	39	0.00	100	0.00	100
3	-1380.521294	6.32		1.83	2	7.58		13.42	
6	-1380.523	4.96		0.86	9	6.24		11.54	
14	-1380.524932	4.04		0.31	23	4.62		7.48	
15	-1380.524932	4.04		0.26	25	4.62		7.48	
31	-1380.522	6.08		1.78	2	7.48		12.86	

[a] Conformers are numbered in the order of appearance in the conformational search.

Table SG2. Total energies (E_{DFT}, in Hartree), relative energies (ΔE_{DFT}, ΔG_{DFT}, $\Delta E_{B2PLYP-D}$, ΔE_{MP2}, in kcal mol^{-1}) and percentage populations of low-energy conformers of **10a** calculated at B2PLYP-D/6-311++G(d,p)//PBE0/6-311++G(d,p) and MP2/6-311++G(d,p)//PBE0/6-311++G(d,p) levels

Conf.[a]	E_{DFT}	ΔE_{DFT}	Pop.	ΔG_{DFT}	Pop.	$\Delta E_{B2PLYP-D}$	Pop.	E_{MP2}	Pop.
1	-1379.91026166	0.00	73	0.76	18	0.00	92	0.00	62
6	-1379.90918744	0.67	23	0.00	68	2.16		0.32	36
14	-1379.90749201	1.74	4	0.95	14	1.42	8	1.97	2

[a] Conformers are numbered in the order of appearance in the conformational search.

Table SG3. Total energies (E_{DFT}, in Hartree), relative energies (ΔE_{DFT}, ΔG_{DFT}, $\Delta E_{B2PLYP-D}$, ΔE_{MP2}, in kcal mol^{-1}) and percentage populations of low-energy conformers of **10a** calculated at B2PLYP-D/6-311++G(d,p)//LC-wPBE/6-311++G(d,p) and MP2/6-311++G(d,p)//LC-wPBE/6-311++G(d,p) levels

Conf.[a]	E_{DFT}	ΔE_{DFT}	Pop.	ΔG_{DFT}	Pop.	$\Delta E_{B2PLYP-D}$	Pop.	E_{MP2}	Pop.
1	-1380.519522	0.00	75	1.07	13	0.00	92	0.00	71
6	-1380.51835	0.74	22	0.00	80	2.17		2.89	
14	-1380.516679	1.78	3	1.48	4	1.46	8	0.53	29

[a] Conformers are numbered in the order of appearance in the conformational search.

Table SG4. Total energies (E_{DFT}, in Hartree), relative energies (ΔE_{DFT}, ΔG_{DFT}, $\Delta E_{B2PLYP-D}$, ΔE_{MP2}, in kcal mol^{-1}) and percentage populations of low-energy conformers of **10a** calculated at B2PLYP-D/6-311++G(d,p)//M06-2X/6-311++G(d,p) and MP2/6-311++G(d,p)//M06-2X/6-311++G(d,p) levels

Conf.[a]	E_{DFT}	ΔE_{DFT}	Pop.	ΔG_{DFT}	Pop.	$\Delta E_{B2PLYP-D}$	Pop.	E_{MP2}	Pop.
1	-1380.970319	0.00	93	0.20	39	0.00	92	0.00	72
6	-1380.966442	2.43		1.56	4	3.14		5.41	
15	-1380.9679	1.52	7	0.00	55	1.47	8	0.81	18
28	-1372.918014	1.14	10	2.05		2.05		1.14	10
32	-1380.966537	2.37		1.81	2	2.95		2.49	

[a] Conformers are numbered in the order of appearance in the conformational search.

Table SH1. Values of dihedral angles α, β, γ, σ and δ (in degrees) for low-energy conformers of **1a**, **2a**, **6a**-**10a** calculated at the LC-wPBE level

Conf.[a]	Dihedral angle[b]								
	α	α′	β	β′	γ	γ′	σ	σ'	δ
1a (2)	80.4	81.0	-179.0	179.9	161.5	158.4	-19.2	-23.0	-61.7
1a (16)	116.8	85.1	173.1	-177.9	-24.1	171.7	158.4	-8.6	-56.7
1a (17)	120.6	121.3	-175.7	-178.8	-168.0	174.2	13.5	-5.4	161.9
1a (23)	115.1	87.7	176.9	178.6	-19.8	165.5	162.3	-15.6	-58.2
1a (25)	-115.0	84.2	-178.5	178.5	172.2	156.4	-8.6	-25.6	-63.8
1a (26)	82.3	-109.7	-179.4	-175.8	161.1	163.4	-19.8	-17.6	-61.7
1a (28)	-115.1	-106.6	-177.8	-176.3	172.2	159.4	-8.6	-22.2	-62.7
1a (32)	121.7	-92.9	-176.7	-179.1	-166.9	176.1	14.8	-3.4	-163.1
1a (33)	-121.9	122.8	-177.1	179.8	-166.8	173.3	14.3	-6.6	-163.5
2a (1)[c]	86.2		178.7		58.5		171.1		-122.2
2a (2)	-108.7	87.0	-172.8	178.4	61.6	58.3	169.8	-118.0	-122.5
2a (3)	-89.8	86.5	179.3	179.8	-108.6	55.1	-176.4	70.1	-126.0
2a (4)	108.1	86.3	176.2	179.5	-110.8	54.6	-176.9	67.8	-126.6
6a (18)[c]	119.8		-178.4		142.8		-36.8		-143.1
6a (22)	93.1	-122.2	-179.9	179.3	143.2	145.3	-36.7	-34.9	-144.2
6a (23)	90.4	-93.9	-178.6	179.3	139.8	-36.4	-39.7	143.7	-140.5
6a (24)	-121.1	120.6	178.4	179.5	147.6	144.9	-32.9	-35.1	-144.6
6a (26)	90.6	89.4	90.6	179.9	141.3	-39.1	-38.5	140.9	-140.6
6a (36)	-117.6	89.5	-179.8	-179.8	144.6	-38.7	-35.6	151.4	-140.9
7a (3)	117.6	-122.8	177.1	177.7	173.2	176.5	-8.4	-5.2	-102.4
7a (7)	120.0	89.0	178.7	-178.8	-172.7	154.9	6.9	-26.3	-99.5
7a (8)	91.4	-120.2	179.5	179.2	165.2	-175.6	-16.3	3.5	-100.1
7a (14)	89.6		178.7		172.5		-8.9		-101.0
7a (18)	-120.2	-127.9	177.4	178.0	162.0	52.7	-20.2	-127.4	-100.9
7a (25)	-125.4	88.4	177.5	180.0	55.8	142.6	-124.3	-38.3	-99.0
7a (26)	88.4	117.6	178.8	176.2	162.8	-178.1	-18.9	0.7	-101.8
7a (32)	122.4	-107.3	-178.9	-178.2	66.6	125.6	-112.4	-54.2	-99.9
7a (35)[c]	-120.6		177.5		179.6		-2.1		-102.2

8a (2)[c]	81.4		-177.5		159.3		-21.1		-69.9
8a (4)	-101.9	131.2	-179.9	175.2	155.9	44.1	-26.0	-137.3	-89.9
8a (6)	86.0	-114.6	-178.6	-178.5	151.5	177.4	-29.9	-2.7	-72.3
8a (9)	-136.1	-136.0	-177.3	178.2	-45.3	49.6	137.2	-131.5	-89.0
8a (11)	-127.1	-85.0	179.3	-176.7	64.8	-42.4	-114.5	140.2	-93.6
8a (12)	119.5	85.1	178.6	175.2	54.1	139.3	-126.2	-42.9	-99.0
8a (14)	-138.9	-91.7	175.8	-1.7	46.3	156.0	-135.4	-25.9	-92.4
8a (24)	-91.6	-92.2	-177.2	-175.3	64.5	-44.1	-114.5	138.8	-87.9
8a (27)	93.9	-95.5	174.5	-178.1	-60.2	-59.6	118.8	120.3	-66.8
9a (2)[c]	81.9		179.4		158.5		-23.0		-60.0
9a (11)	-107.5	83.4	-175.5	179.7	161.5	158.4	-19.7	-23.2	-59.6
9a (19)	117.2	88.2	177.0	179.0	-21.2	165.5	161.5	-15.7	-56.6
10a (1)[c]	81.8		178.2		156.8		-25.3		-55.6
10a (6)	82.4	-112.1	179.5	-175.9	158.4	156.2	-23.4	-25.6	-54.5
10a (14)	87.0	121.7	178.7	177.9	165.7	-26.6	-15.8	156.9	-51.7

[a] Conformers are numbered in the order of appearance in the conformational search; [b] α, α' = C9-C1-O-C(=O); β, β' = C1-O-C(=O)-C; γ, γ' = O-C(=O)-C*-C*; δ = (O=)C-C*-C*-C(=O); [c] C_2-symmetry; [d] σ, σ' = O=C-C*-C*.

Table SH2. Distances and angles τ, ψ and *ω* between electronic transition dipole moments polarized along the long axis of naphthalene chromophore (in degrees), estimated rotatory strengths (*R*) based on Norden's and Rodger's geometrical model, long- and short-wavelengths rotatory strengths and amplitudes of rotatory strengths calculated for low-energy conformers of **1a**, **2a**, **6a**-**10a** at the LC-wPBE/6-311++G(d,p) level

Conformer[a]	l[b] [Å]	τ[c] [°]	ψ[d] [°]	ω[e] [°]	*R*[f]	R_{long}	R_{short}	A[g]
1a (conf. 2)	6.701	54	54	79	4.305	1321	-1114	2435
1a (conf. 16)	6.615	50	48	-82	-3.729	778	-697	1475
1a (conf. 17)	11.226	84	83	73	10.597	440	-270	710
1a (conf. 23)	6.730	52	50	87	4.057	947	-905	1852
1a (conf. 25)	8.754	60	39	64	4.288	729	-743	1472
1a (conf. 26)	8.447	38	59	76	4.325	726	-712	1438
1a (conf. 28)	10.203	45	43	57	4.127	467	-679	1146
1a (conf. 32)	11.446	74	77	54	8.673	142	-54	196
1a (conf. 33)	11.614	76	67	21	3.717	110	-82	192
2a (conf. 1)	10.424	81	81	-78	-9.947	-137	170	-307
2a (conf. 2)	10.468	78	82	-81	-10.015	-254	293	-547
2a (conf. 3)	10.458	90	81	-55	-8.461	-390	362	-752
2a (conf. 4)	10.453	82	82	-45	-7.248	-569	611	-1180
6a (conf. 18)	9.193	69	69	23	3.131	667	-388	1055
6a (conf. 22)	10.368	59	74	-74	-8.212	-205	147	-352
6a (conf. 23)	9.183	81	67	-64	-7.504	-840	785	-1625
6a (conf. 24)	10.673	56	84	-41	-5.773	-190	234	-424
6a (conf. 26)	10.466	55	88	-64	-7.701	-300	253	-553
6a (conf. 36)	10.853	76	59	-77	-8.795	-313	363	-676
7a (conf. 3)	10.983	88	51	50	6.534	218	-148	366
7a (conf. 7)	9.491	66	85	80	8.506	407	-185	592
7a (conf. 8)	10.999	49	77	34	4.523	351	-387	738
7a (conf. 14)	9.209	70	70	57	6.820	949	-755	1704
7a (conf. 18)	8.956	36	88	32	2.788	313	-366	679

7a (conf. 25)	6.520	45	81	55	3.730	2018	-932	2950
7a (conf. 26)	9.667	89	69	75	8.716	555	-333	888
7a (conf. 32)	7.464	45	57	65	4.012	-337	428	-765
7a (conf. 35)	11.579	63	63	4	0.641	54	-262	316
8a (conf. 2)	6.966	53	53	73	4.249	1391	-1197	2588
8a (conf. 4)	7.667	74	27	55	2.741	527	-483	1010
8a (conf. 6)	8.987	60	42	56	4.317	72	-749	821
8a (conf. 11)	6.536	53	81	82	5.105	-187	223	-410
8a (conf. 12)	6.215	61	75	64	4.719	258	-279	537
8a (conf. 14)	5.960	47	73	-69	-3.891	-989	865	-1854
8a (conf. 24)	6.757	48	83	62	4.401	703	-657	1360
8a (conf. 27)	8.563	65	47	78	5.552	-240	304	-544
9a (conf. 2)	6.647	54	54	80	4.284	1329	-1124	2453
9a (conf. 11)	8.311	38	58	79	4.259	772	-710	1482
9a (conf. 19)	6.598	54	49	90	4.029	892	-798	1690
10a (conf. 1)	6.605	54	54	82	4.281	1382	-1115	2497
10a (conf. 6)	8.240	58	33	78	3.723	769	-676	1445
10a (conf. 14)	6.512	48	55	-87	-3.959	896	-718	1614

[a] Conformers are numbered in the order of appearance in the conformational search; [b] measured between the midpoints of dipoles; [c] τ = a-c-c' or b-c-c' and $0° < \tau \leq 90°$; [d] ψ = a'-c'-c or b'-c'-c and $0° < \psi \leq 90°$ [e] ω = a-c-c'-a' or b-c-c'-a' or a-c-c'-b' or b-c-c'-b' and $0° < |\omega| < 180°$; [f] R = const l sinτ sinψ sinω [g] A = R_{long} – R_{short}, in 10^{-40} erg esu cm Gauss^{-1}.

Table SI1. Crystal data and data collection, and refinement parameters

	6a	**6b**
Crystal data		
Chemical formula	$C_{25}H_{18}O_4$	
M_r	382.39	
Crystal system, space group	Trigonal, $P3_2$	Monoclinic, $P2_1$
Temperature (K)	150	295
a, b, c (Å)	7.7367 (1), 7.7367 (1), 27.7775 (3)	8.2590 (3), 5.8054 (2), 40.0039 (14)
□, □, □ (°)	90, 90, 120	90, 90.611 (3), 90
V (Å^3)	1439.91 (4)	1917.95 (12)
Radiation type	Cu $K\alpha$	
Z	3	4
□ (mm^{-1})	0.72	0.73
Crystal size (mm)	0.55 × 0.35 × 0.10	0.40 × 0.07 × 0.04
Data collection		
T_{min}, T_{max}	0.784, 1.000	0.789, 1.000
No. of measured, independent and observed [I > 2□(I)] reflections	20729, 3375, 3362	14673, 6157, 4839
R_{int}	0.028	0.035
(sin □/□)$_{max}$ (Å^{-1})	0.595	0.595
Refinement		
$R[F^2 > 2\square(F^2)]$, $wR(F^2)$, S	0.057, 0.161, 1.08	0.045, 0.103, 1.02
No. of reflections	3375	6157
No. of parameters	403	523
No. of restraints	913	1
□ ρ_{max}, □ρ_{min} (e Å^{-3})	0.26, -0.28	0.13, -0.16
Absolute structure parameter	0.01 (7)	0.23 (13)

Table SI2. Torsion and pseudotorsion angles (°) and distances between centroids of the naphthalene rings (Å) as found in the crystal structures of **6a** and **6b**. For definition of the used notation, see Figures 2 and A2)

	6a two independent molecules		**6b** two independent molecules	
α	C19–C11–O2–C4	-97.2(12)	C11–C12–O2–C4	102.0(4)
	C29–C21–O4–C5	82.3(12)	C21–C22–O4–C5	-116.0(4)
	C49–C41–O6–C34	89.7(13)	C41–C42–O6–C34	-128.5(4)
	C59–C51–O8–C35	-104.3(16)	C51–C52–O8–C35	99.4(4)
β	C11–O2–C4–C2	-176.2(9)	C12–O2–C4–C2	-176.1(4)
	C21–O4–C5–C3	-174.5(9)	C22–O4–C5–C3	-174.1(4)
	C41–O6–C34–C2	-171.8(10)	C42–O6–C34–C32	179.2(3)
	C51–O8–C35–C3	-179.9(11)	C52–O8–C35–C33	174.3(3)
γ	O2–C4–C2–C3	-151.6(11)	O2–C4–C2–C3	-157.2(4)
	O4–C5–C3–C2	-134.6(11)	O4–C5–C3–C2	-166.7(4)
	O6–C34–C2–C3	-137.0(13)	O6–C34–C32–C33	15.0(5)
	O8–C35–C3–C2	-149.5(14)	O8–C35–C33–C32	29.0(6)
δ	C4–C2–C3–C5	144.4(10)	C4–C2–C3–C5	148.7(4)
	C34–C2–C3–C35	145.2(11)	C34–C32–C33–C35	143.9(4)
ω	a–c–c'–b'	35.1	a–c–c'–b'	14.8
	b–c–c'–a'	35.1	b–c–c'–a'	-3.7
	a–c–c'–b'	35.6	a–c–c'–b'	-38.1
	b–c–c'–a'	35.5	b–c–c'–a'	-39.9
l	c–c'	10.51	c–c'	13.02
		10.69		12.48

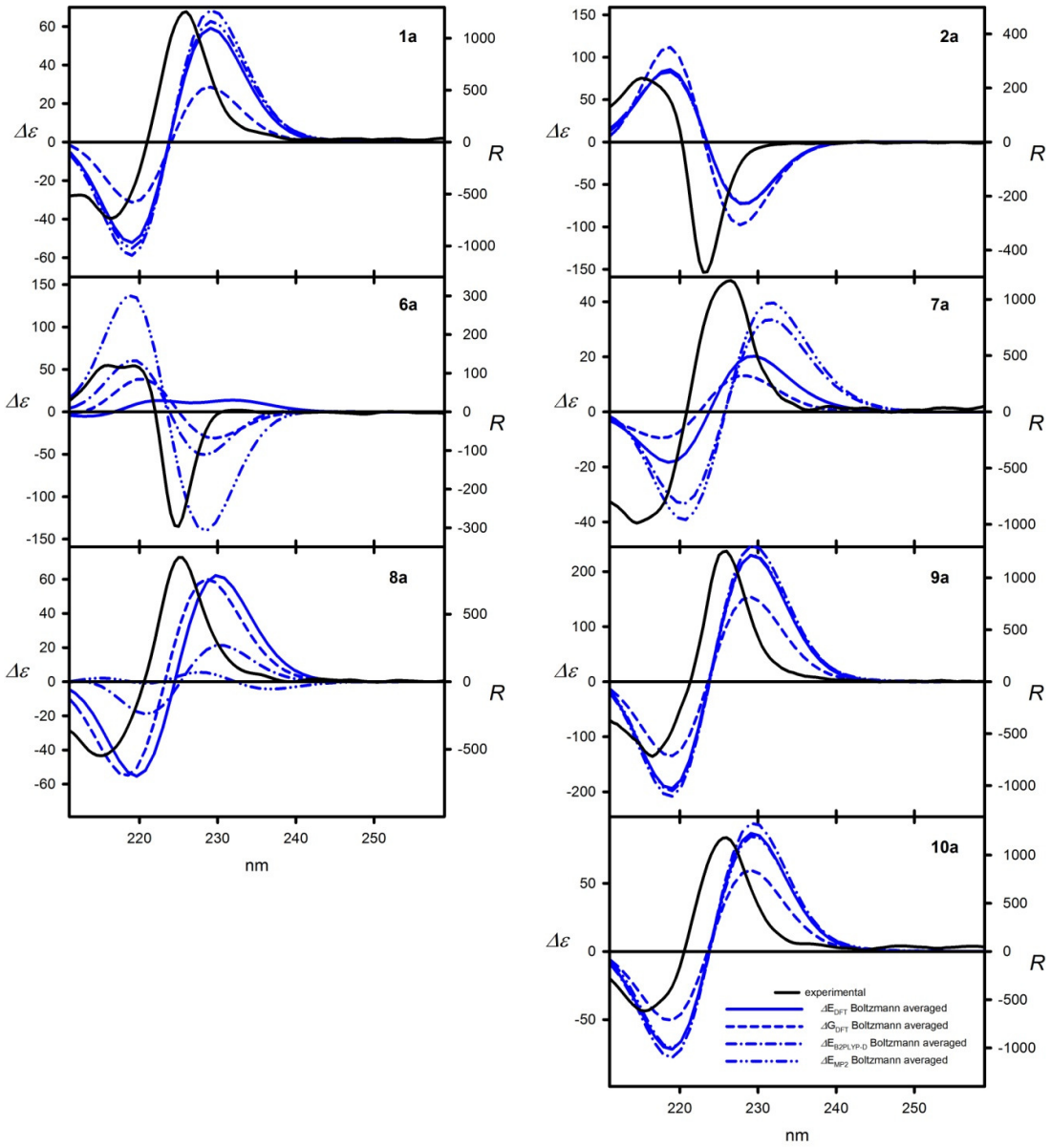

Figure SA1. CD spectra of **1a**, **2a**, **6a**-**10a** experimental (solid black lines) and calculated at the TD-DFT level, ΔE_{DFT}, ΔG_{DFT}, $\Delta E_{B2LYP-D}$ and ΔE_{MP2}-based and Boltzmann averaged (blue lines, geometries optimized at the LC-wPBE/6-311++G(d,p) level). All calculated spectra were wavelength corrected to match the experimental UV spectra.

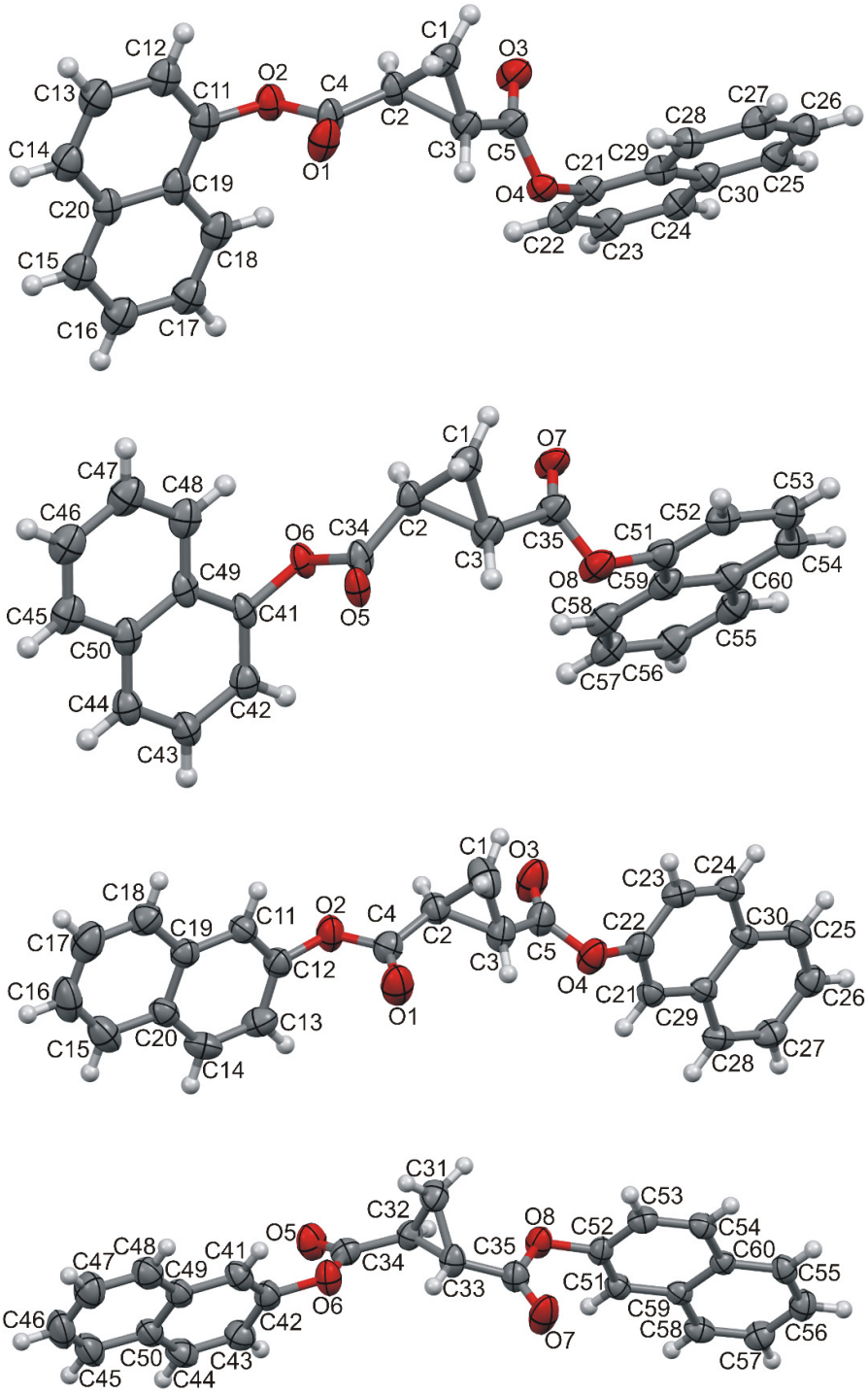

Figure SA2. Perspective view of two independent molecules of **6a** that occupy the same site in crystal (top two molecules). The occupancy factors for the two sites refined to 0.54 and 0.46. Two independent molecules of **6b**, (bottom). Thermal ellipsoids are drawn at 40% probability level. H-atoms are drawn in arbitrary scale.

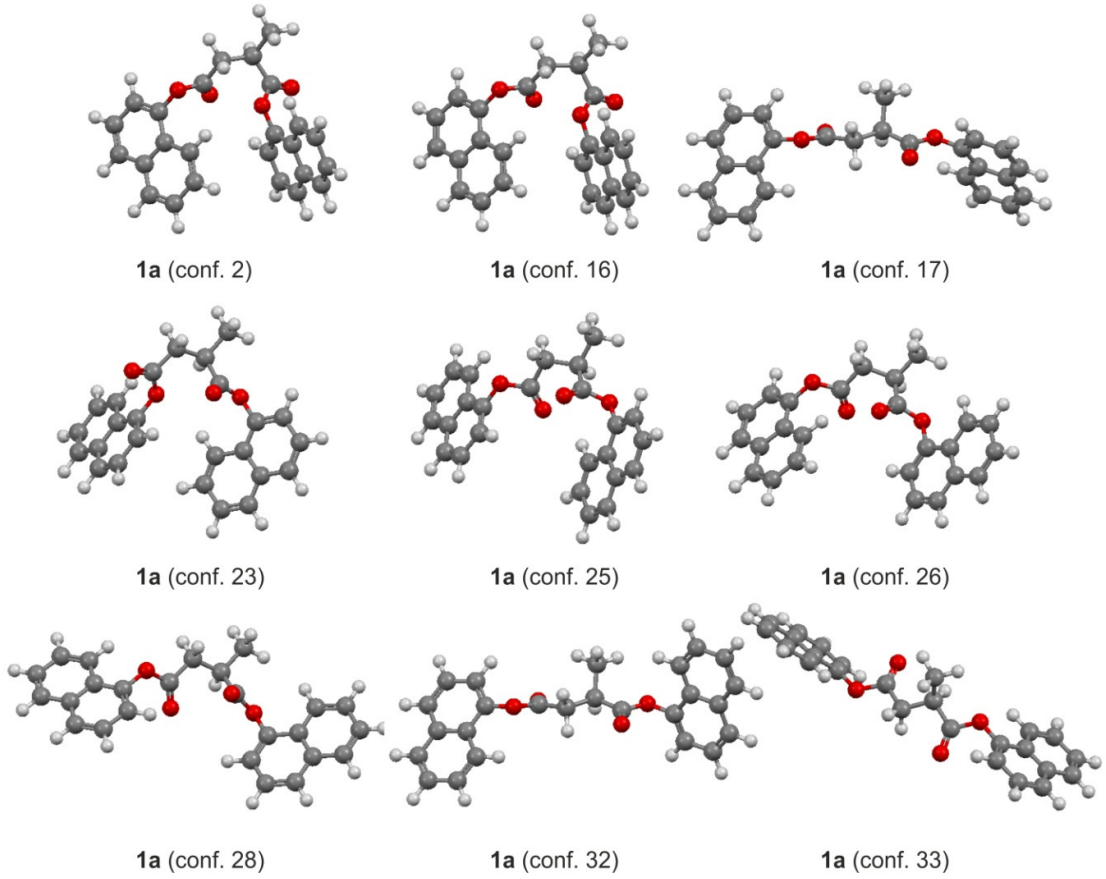

Figure SB1. Structures of low-energy conformers of **1a** calculated at the LC-wPBE/6-311++G(d,p) level. Conformers are numbered in the order of appearance in the conformational search.

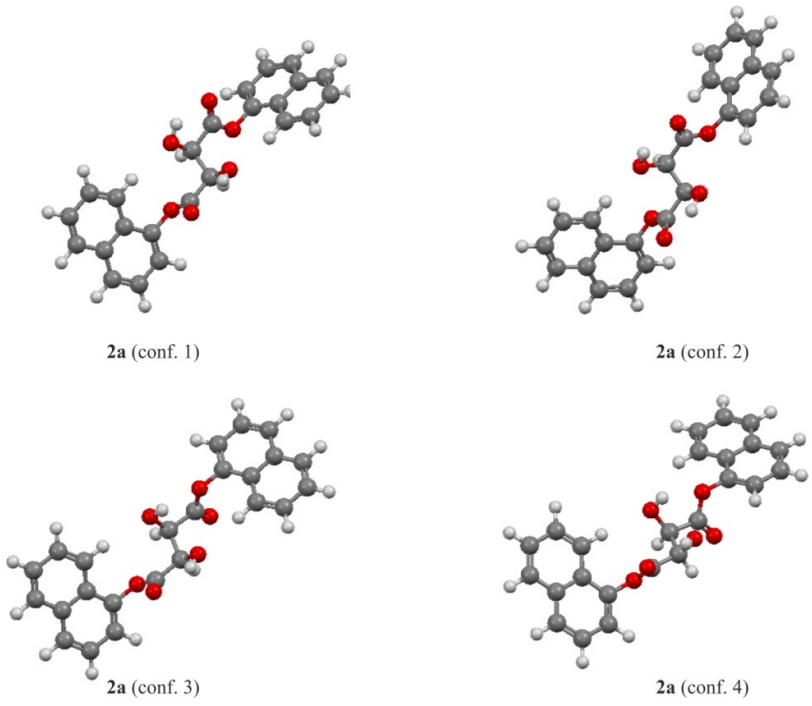

Figure SB2. Structures of low-energy conformers of **2a** calculated at the LC-wPBE/6-311++G(d,p) level. Conformers are numbered in the order of appearance in the conformational search.

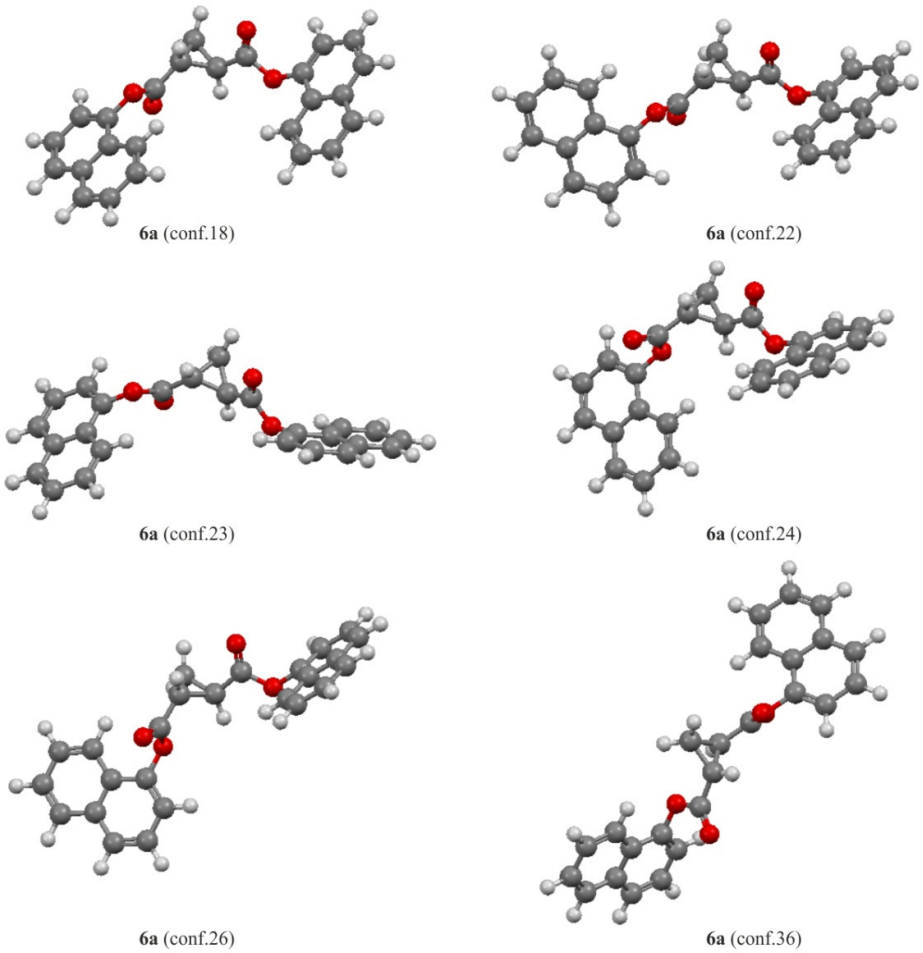

Figure B3. Structures of low-energy conformers of **6a** calculated at the LC-wPBE/6-311++G(d,p) level. Conformers are numbered in the order of appearance in the conformational search.

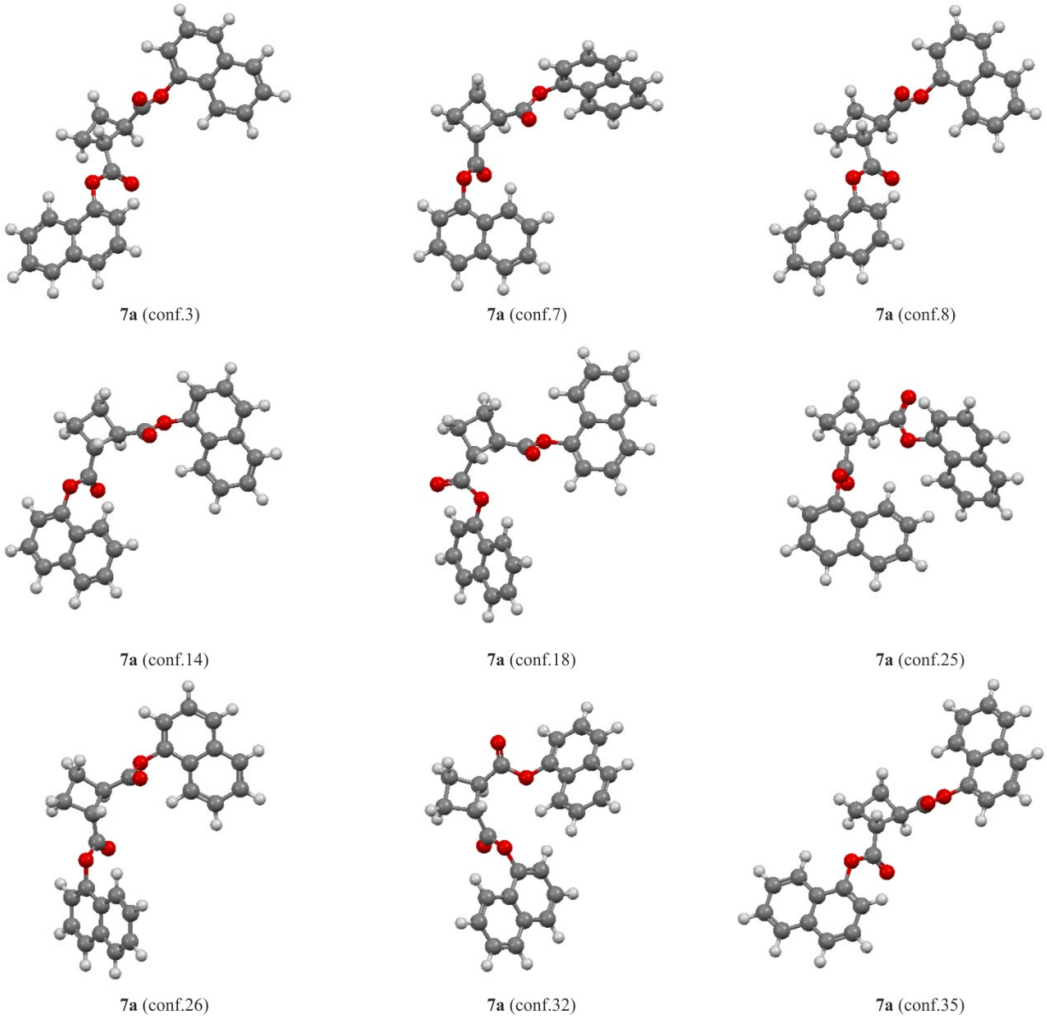

Figure SB4. Structures of low-energy conformers of **7a** calculated at the LC-wPBE/6-311++G(d,p) level. Conformers are numbered in the order of appearance in the conformational search.

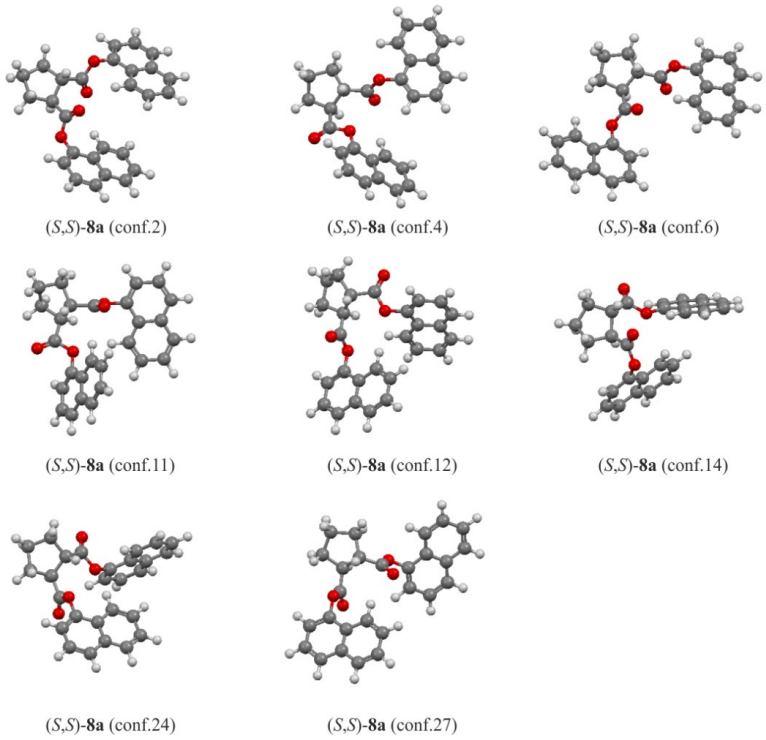

Figure SB5. Structures of low-energy conformers of **8a** calculated at the LC-wPBE/6-311++G(d,p) level. Conformers are numbered in the order of appearance in the conformational search.

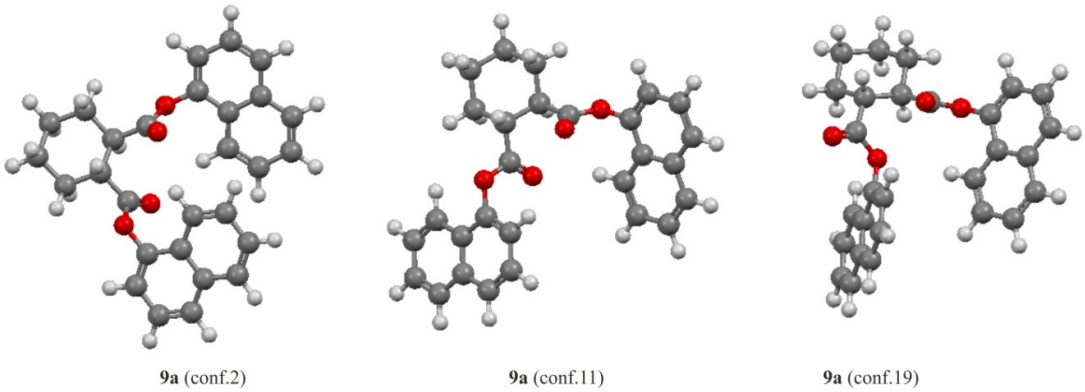

Figure SB6. Structures of low-energy conformers of **9a** calculated at the LC-wPBE/6-311++G(d,p) level. Conformers are numbered in the order of appearance in the conformational search.

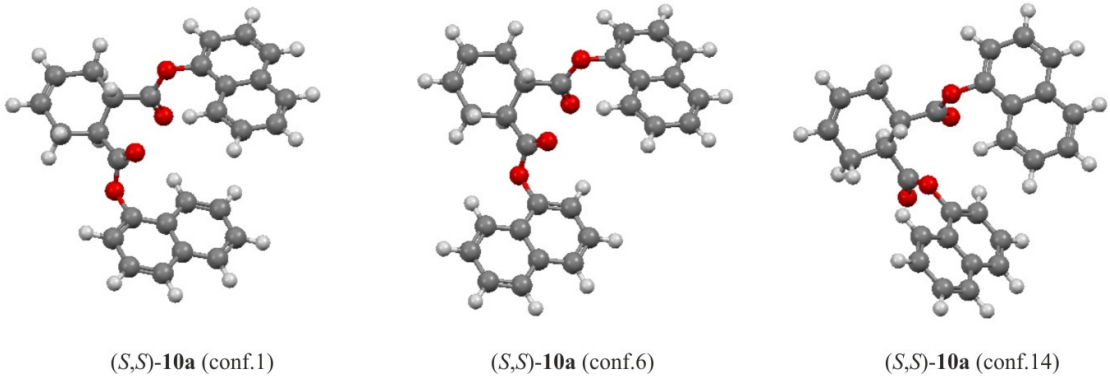

Figure SB7. Structures of low-energy conformers of **10a** calculated at the LC-wPBE/6-311++G(d,p) level. Conformers are numbered in the order of appearance in the conformational search.

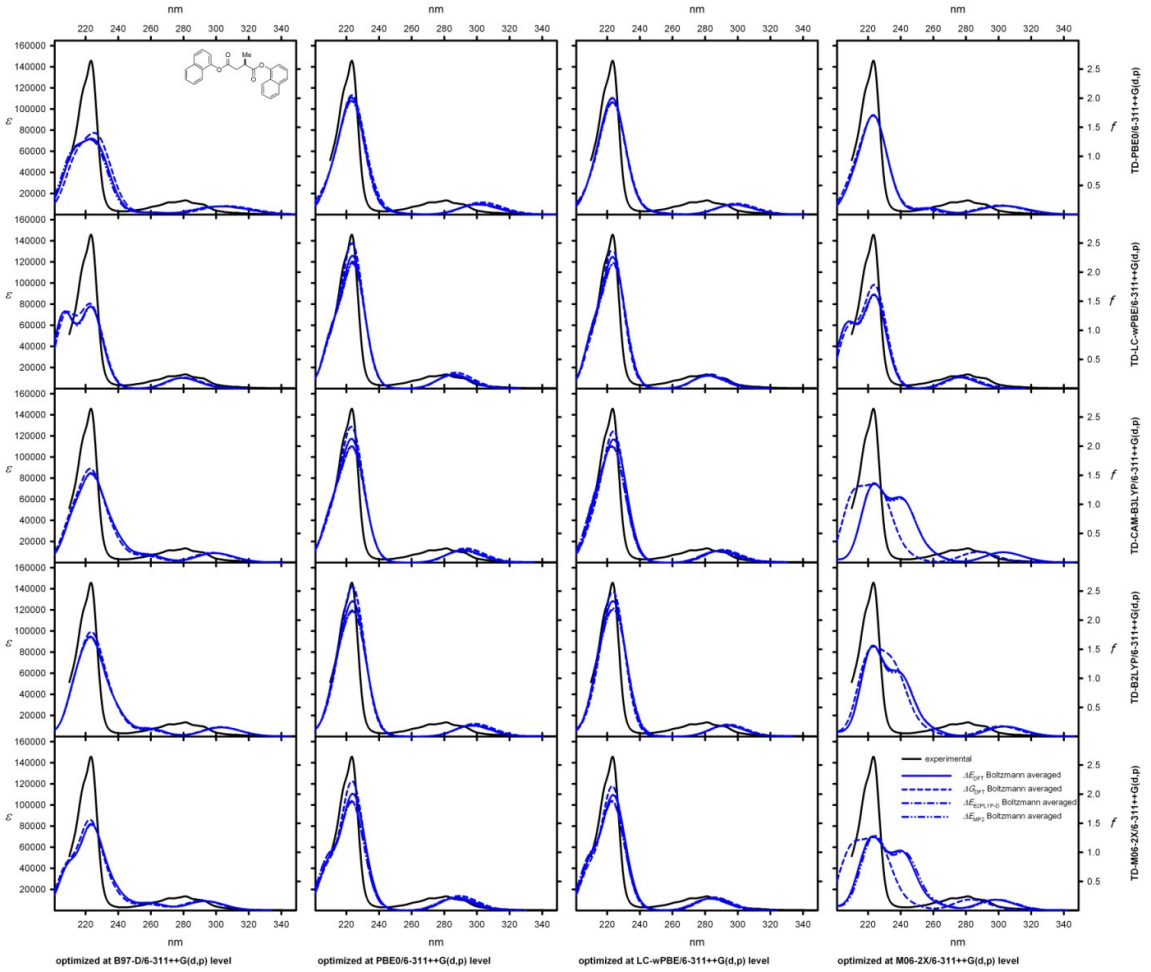

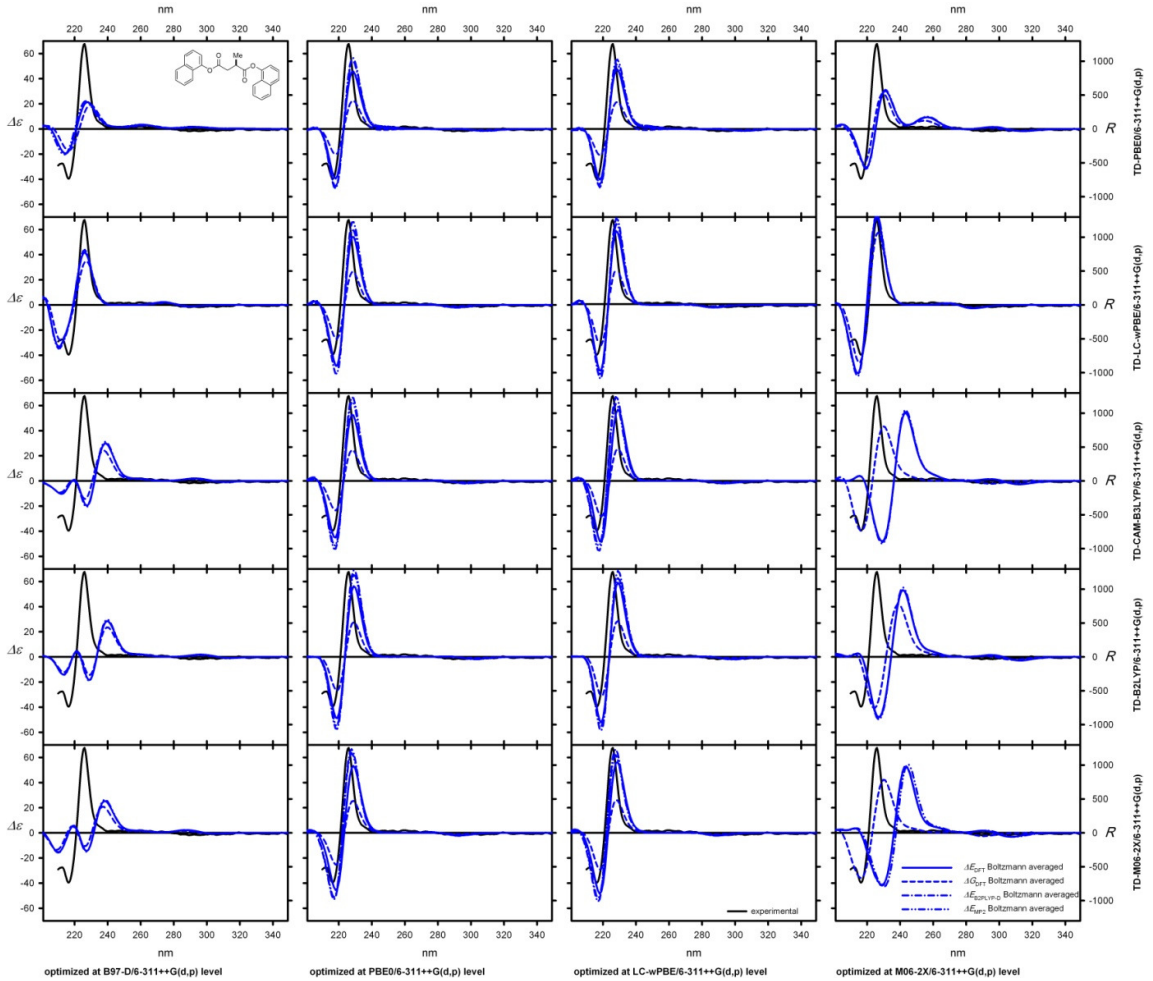

Figure SC1. UV (upper panels) and CD (lower panels) spectra of **1a** experimental (solid black lines) and calculated at the TD-DFT level, ΔE_{DFT}, ΔG_{DFT}, $\Delta E_{B2LYP\text{-}D}$ and ΔE_{MP2}-based and Boltzmann averaged (blue lines, geometries optimized at the DFT/6-311++G(d,p) level). All calculated spectra were wavelength corrected to match the experimental UV spectra.

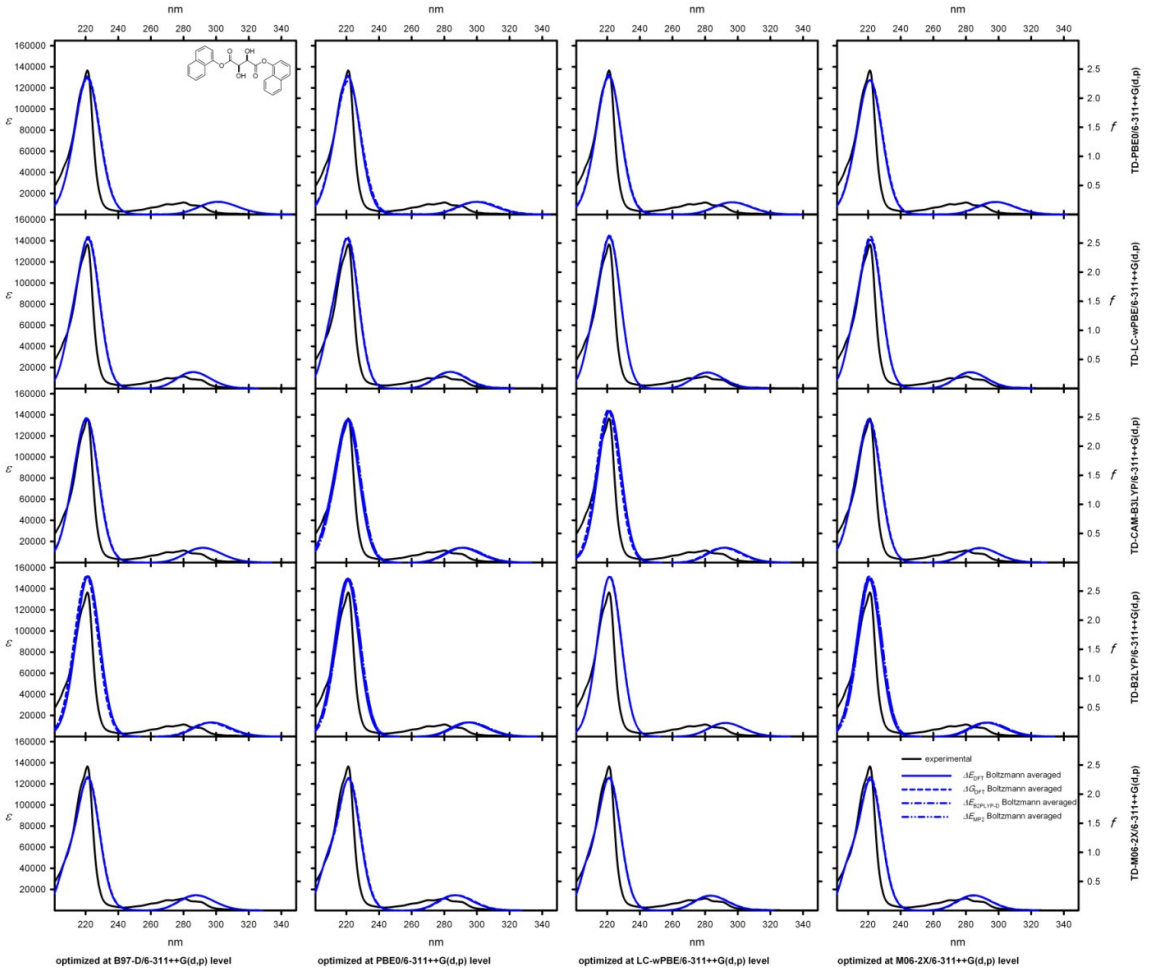

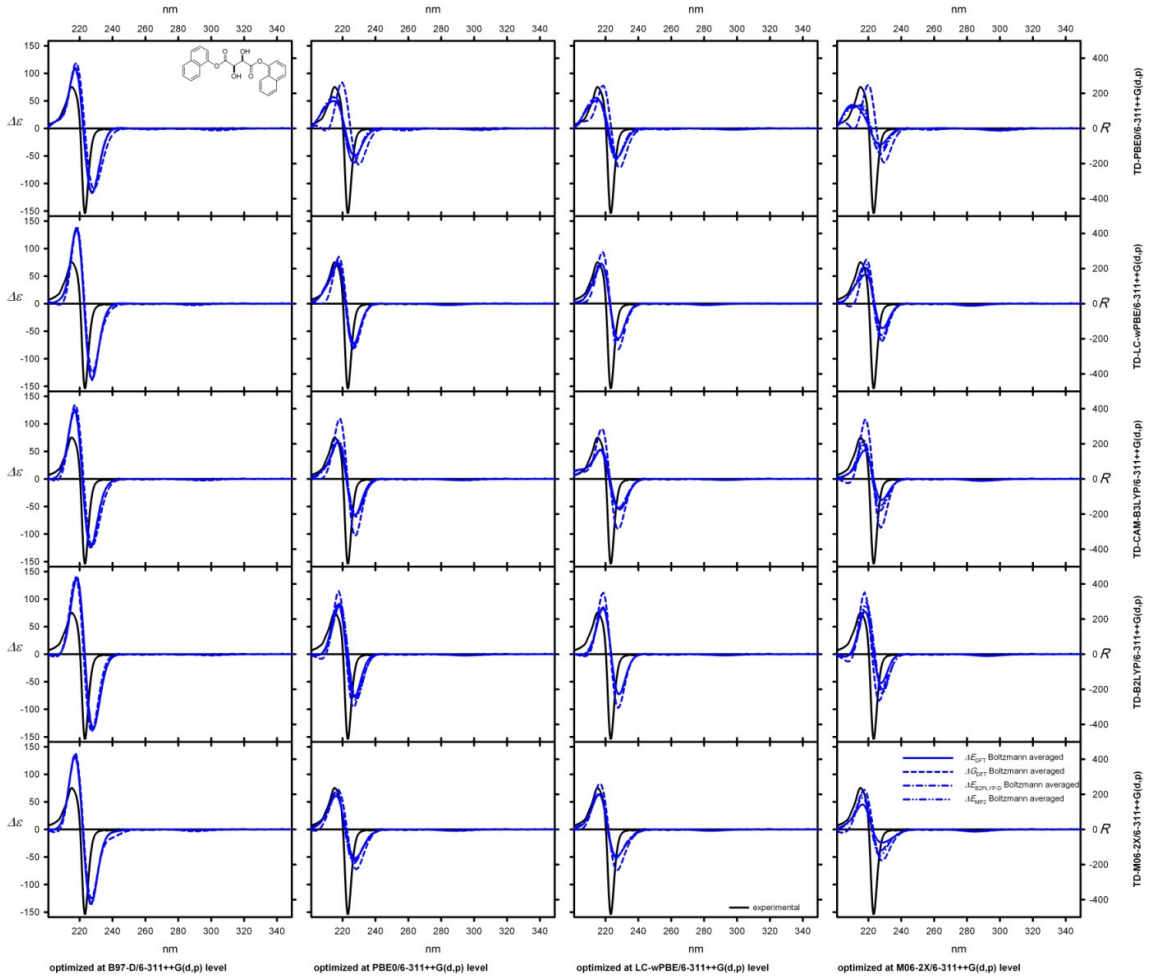

Figure SC2. UV (upper panels) and CD (lower panels) spectra of **2a** experimental (solid black lines) and calculated at the TD-DFT level, ΔE_{DFT}, ΔG_{DFT}, $\Delta E_{B2LYP-D}$ and ΔE_{MP2}-based and Boltzmann averaged (blue lines, geometries optimized at the DFT/6-311++G(d,p) level). All calculated spectra were wavelength corrected to match the experimental UV spectra.

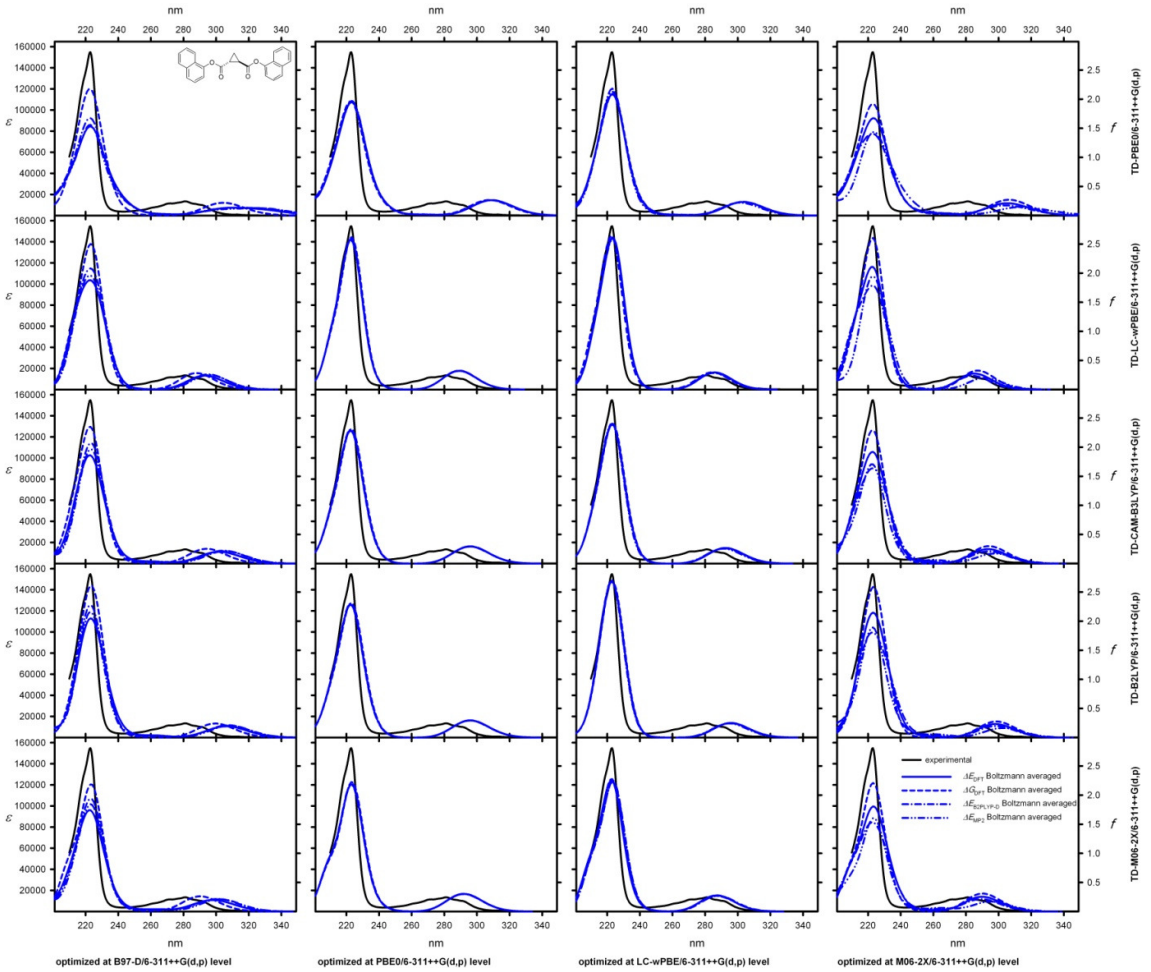

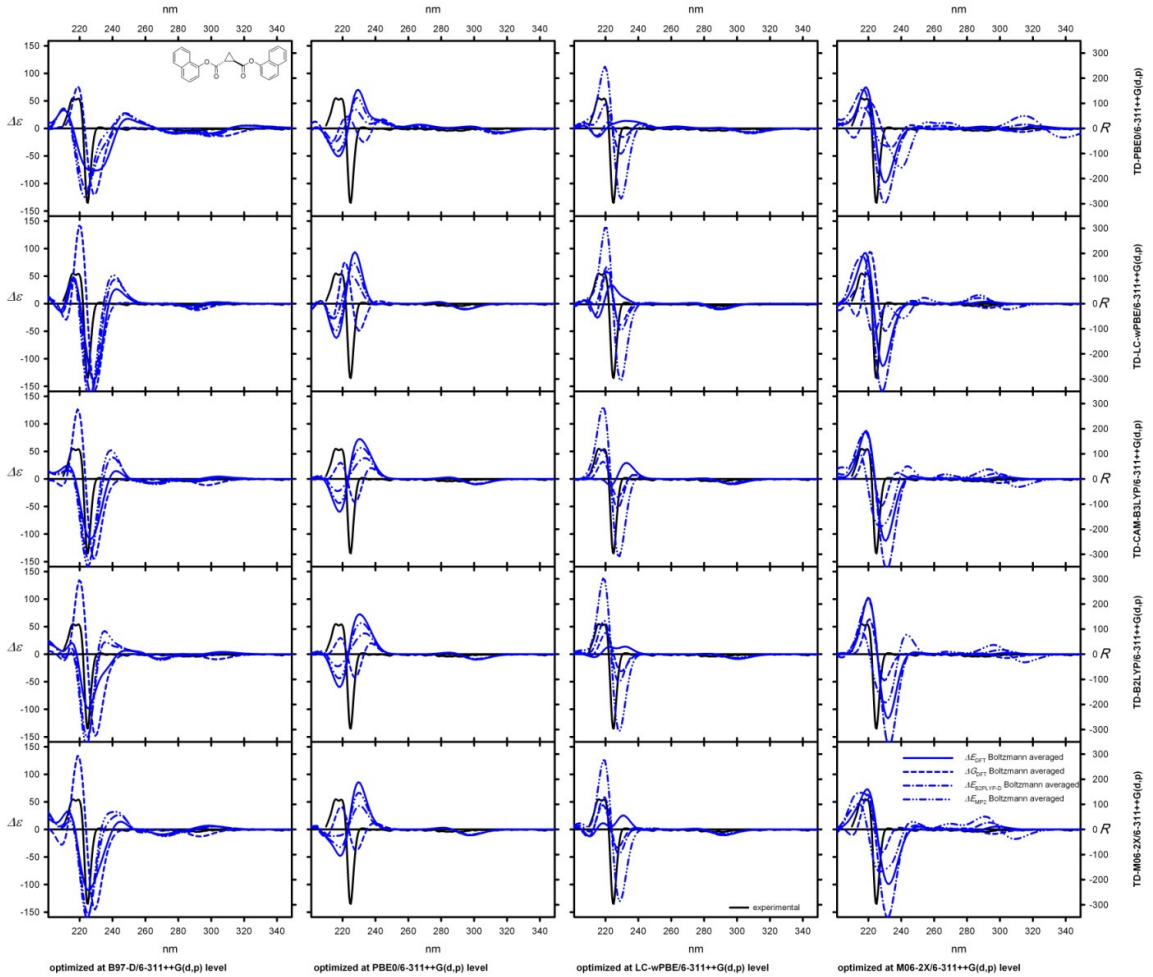

Figure SC3. UV (upper panels) and CD (lower panels) spectra of **6a** experimental (solid black lines) and calculated at the TD-DFT level, ΔE_{DFT}, ΔG_{DFT}, $\Delta E_{B2LYP-D}$ and ΔE_{MP2}-based and Boltzmann averaged (blue lines, geometries optimized at the DFT/6-311++G(d,p) level). All calculated spectra were wavelength corrected to match the experimental UV spectra.

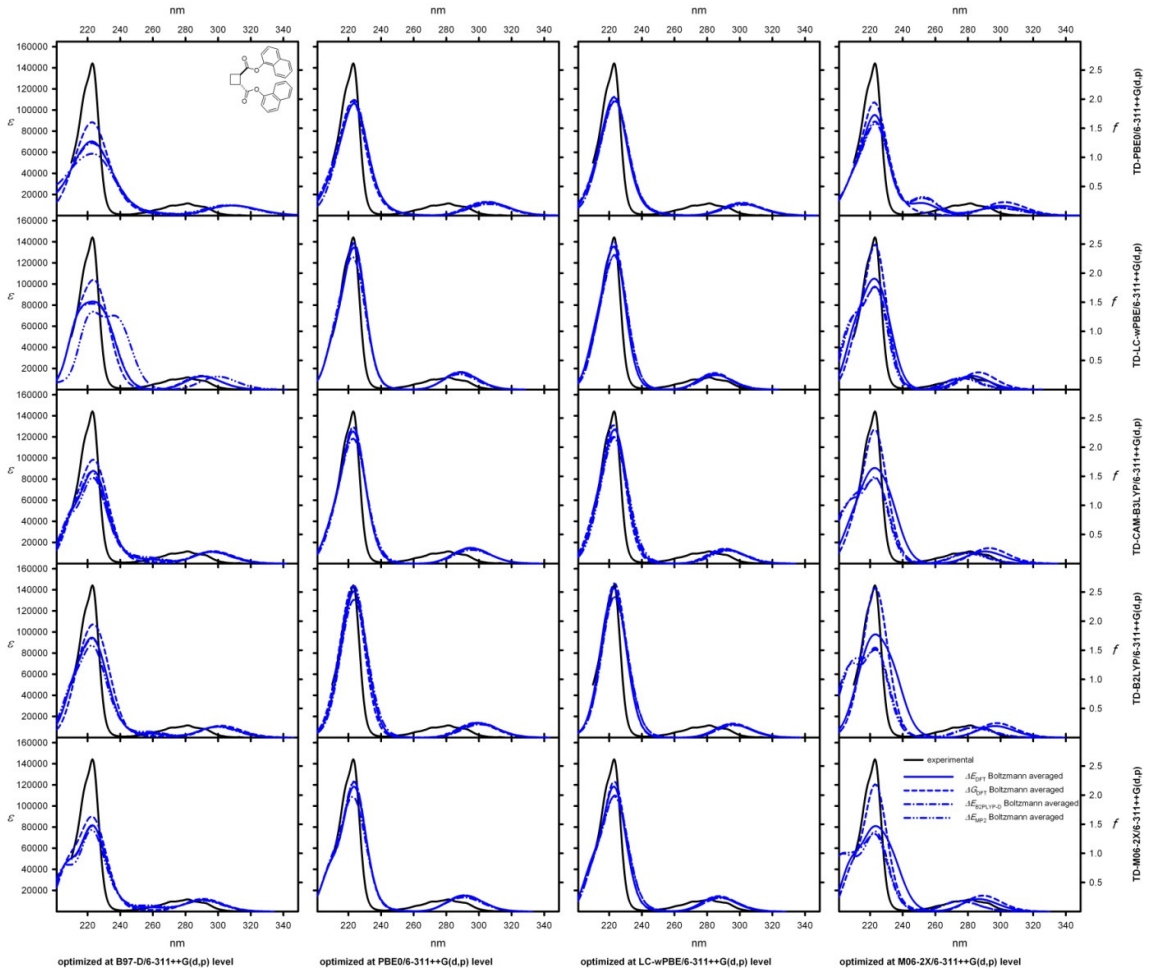

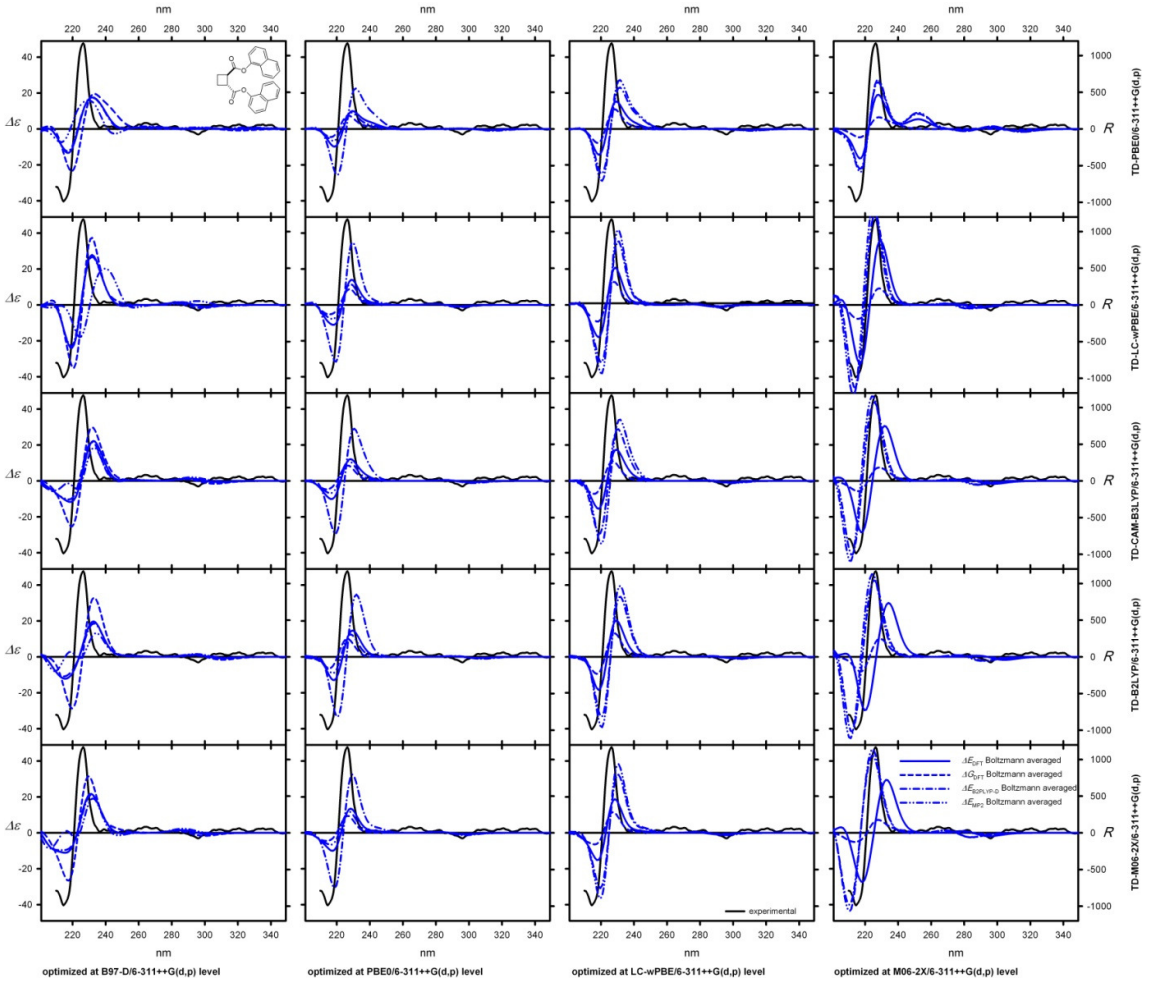

Figure SC4. UV (upper panels) and CD (lower panels) spectra of **7a** experimental (solid black lines) and calculated at the TD-DFT level, ΔE_{DFT}, ΔG_{DFT}, $\Delta E_{B2LYP\text{-}D}$ and ΔE_{MP2}-based and Boltzmann averaged (blue lines, geometries optimized at the DFT/6-311++G(d,p) level). All calculated spectra were wavelength corrected to match the experimental UV spectra.

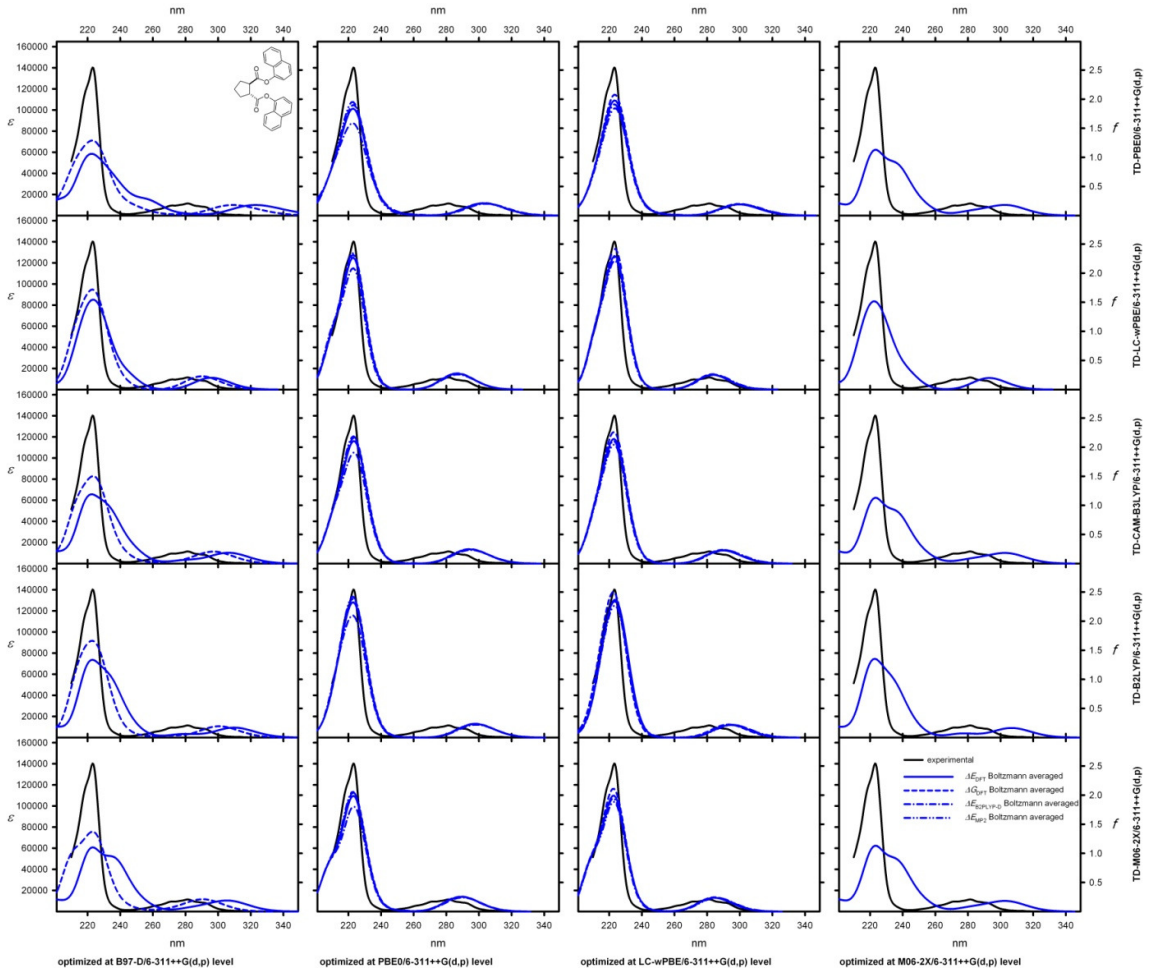

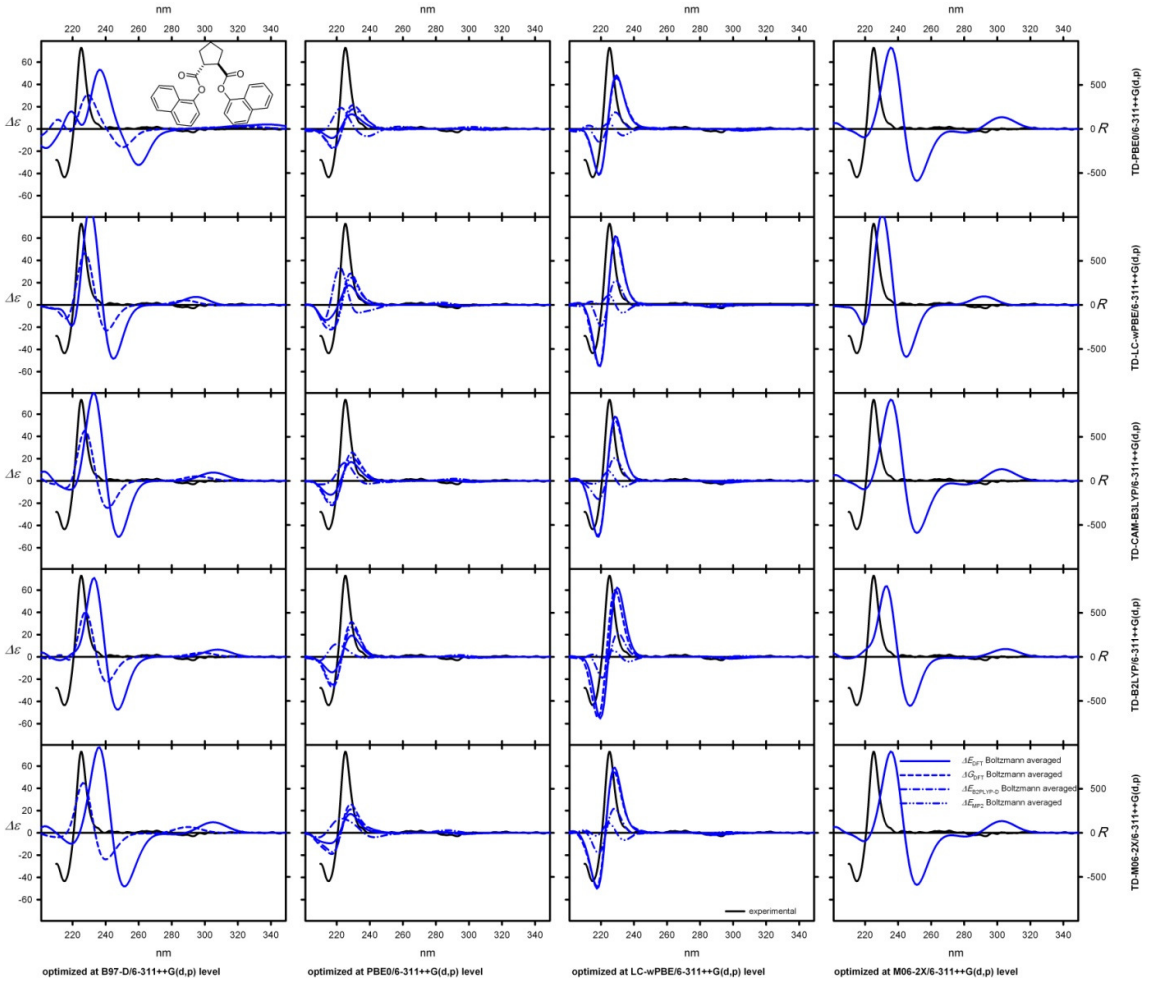

Figure SC5. UV (upper panels) and CD (lower panels) spectra of **8a** experimental (solid black lines) and calculated at the TD-DFT level, ΔE_{DFT}, ΔG_{DFT}, $\Delta E_{B2LYP\text{-}D}$ and ΔE_{MP2}-based and Boltzmann averaged (blue lines, geometries optimized at the DFT/6-311++G(d,p) level). All calculated spectra were wavelength corrected to match the experimental UV spectra.

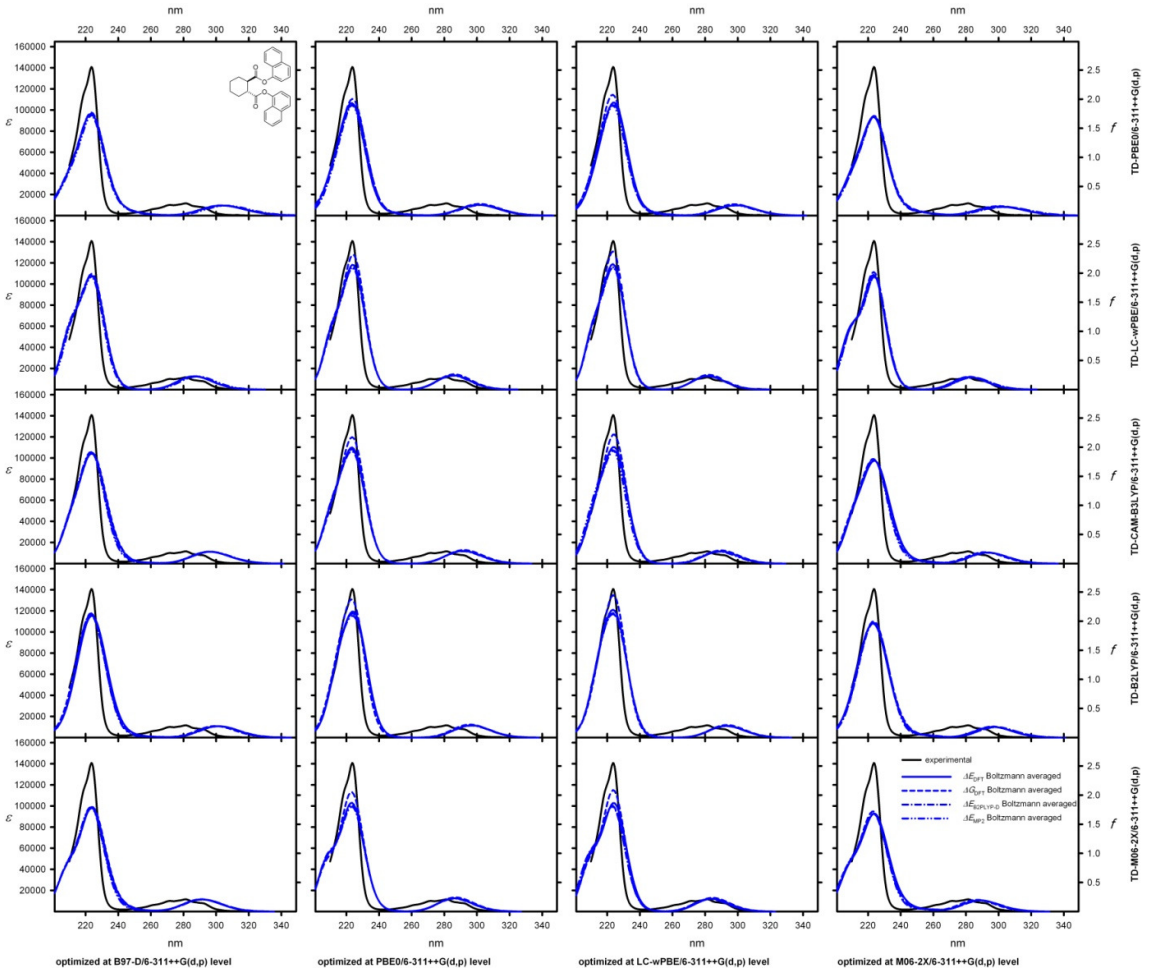

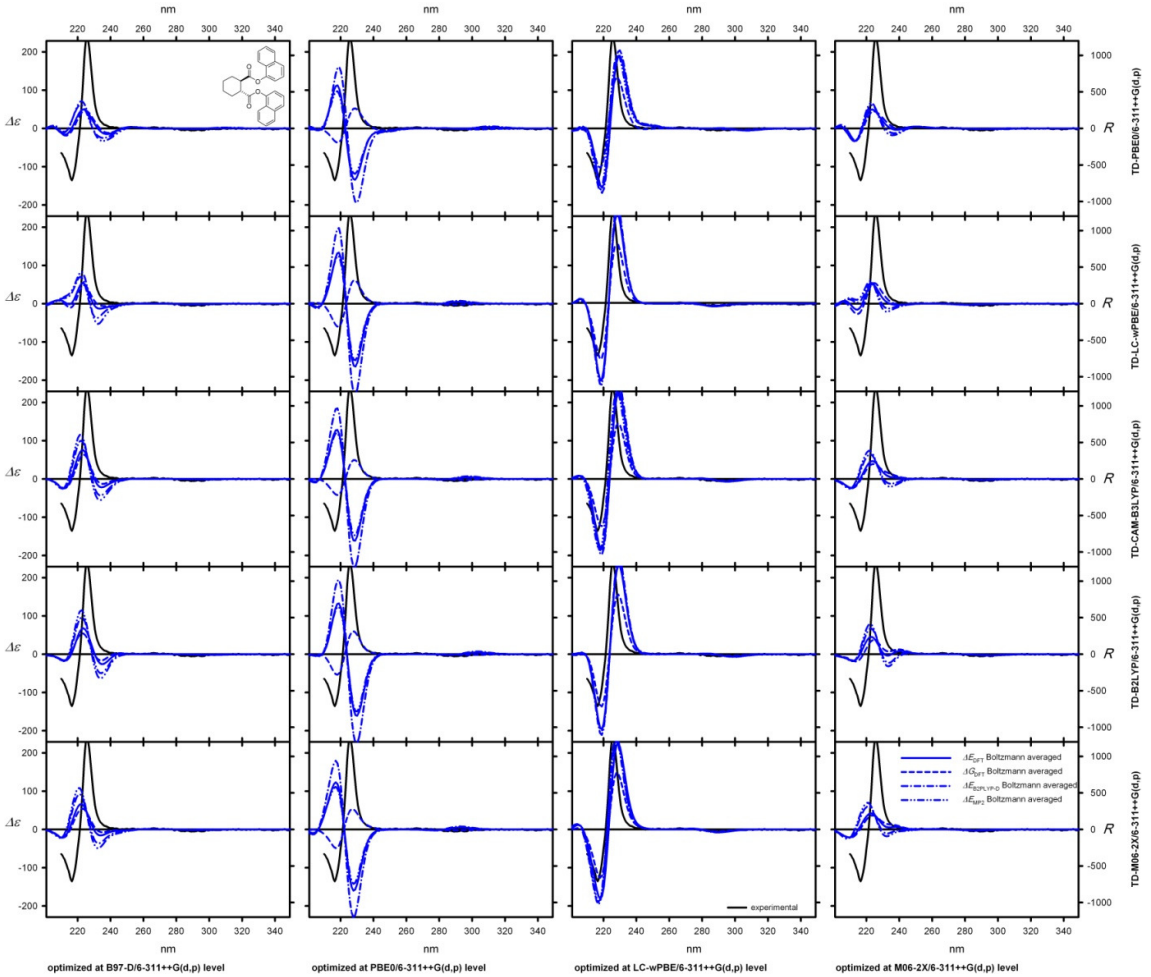

Figure SC6. UV (upper panels) and CD (lower panels) spectra of **9a** experimental (solid black lines) and calculated at the TD-DFT level, ΔE_{DFT}, ΔG_{DFT}, $\Delta E_{B2LYP-D}$ and ΔE_{MP2}-based and Boltzmann averaged (blue lines, geometries optimized at the DFT/6-311++G(d,p) level). All calculated spectra were wavelength corrected to match the experimental UV spectra.

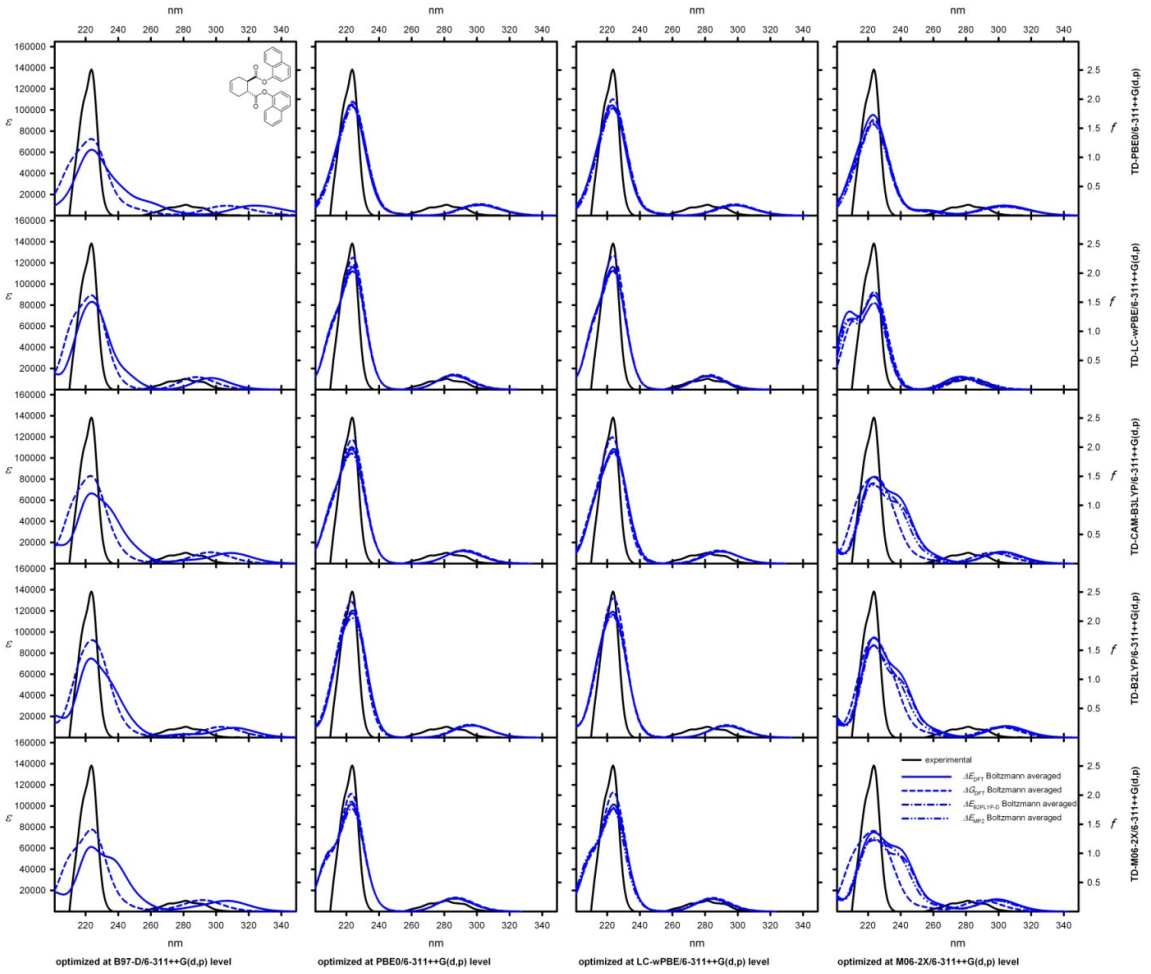

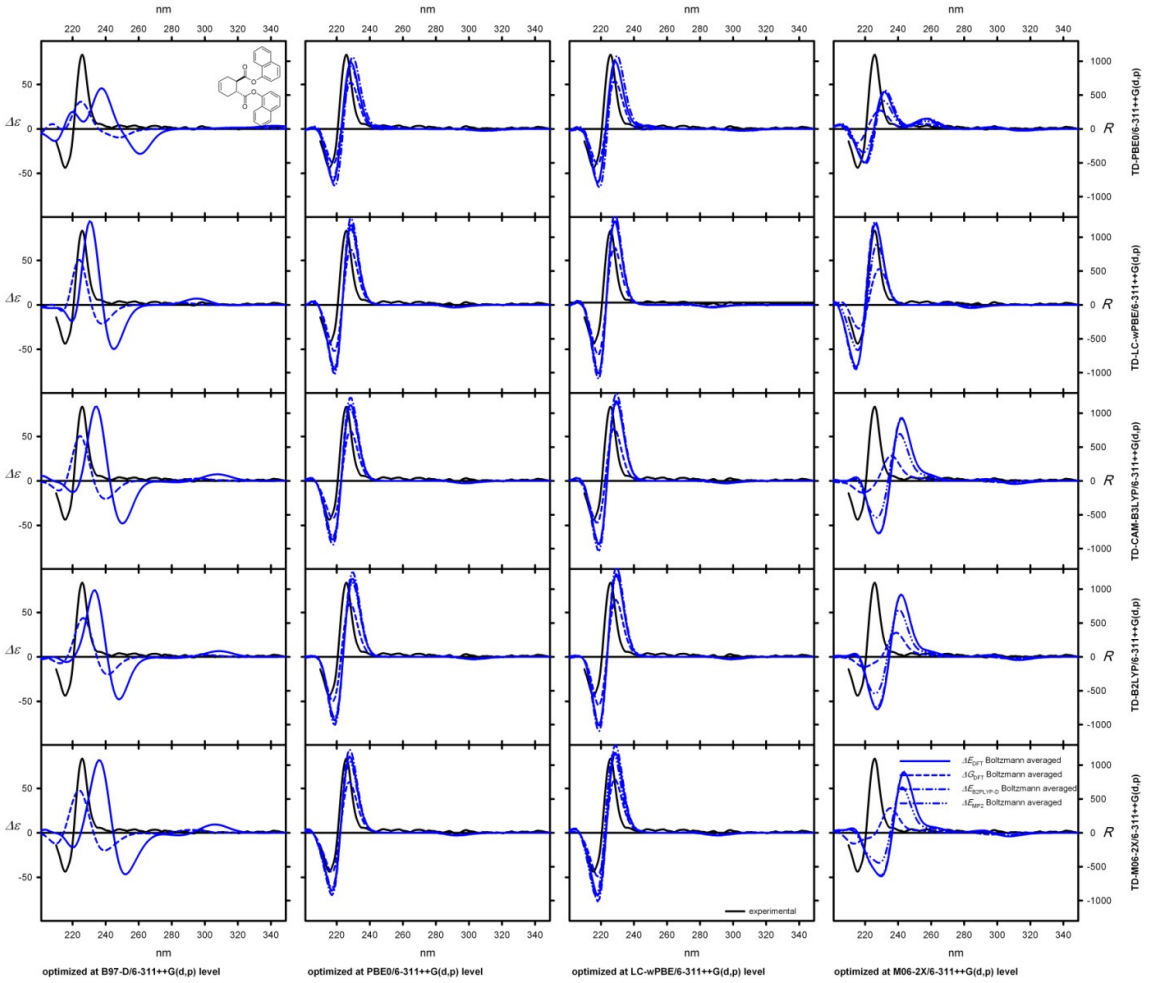

Figure SC7. UV (upper panels) and CD (lower panels) spectra of **10a** experimental (solid black lines) and calculated at the TD-DFT level, ΔE_{DFT}, ΔG_{DFT}, $\Delta E_{B2LYP\text{-}D}$ and ΔE_{MP2}-based and Boltzmann averaged (blue lines, geometries optimized at the DFT/6-311++G(d,p) level). All calculated spectra were wavelength corrected to match the experimental UV spectra.

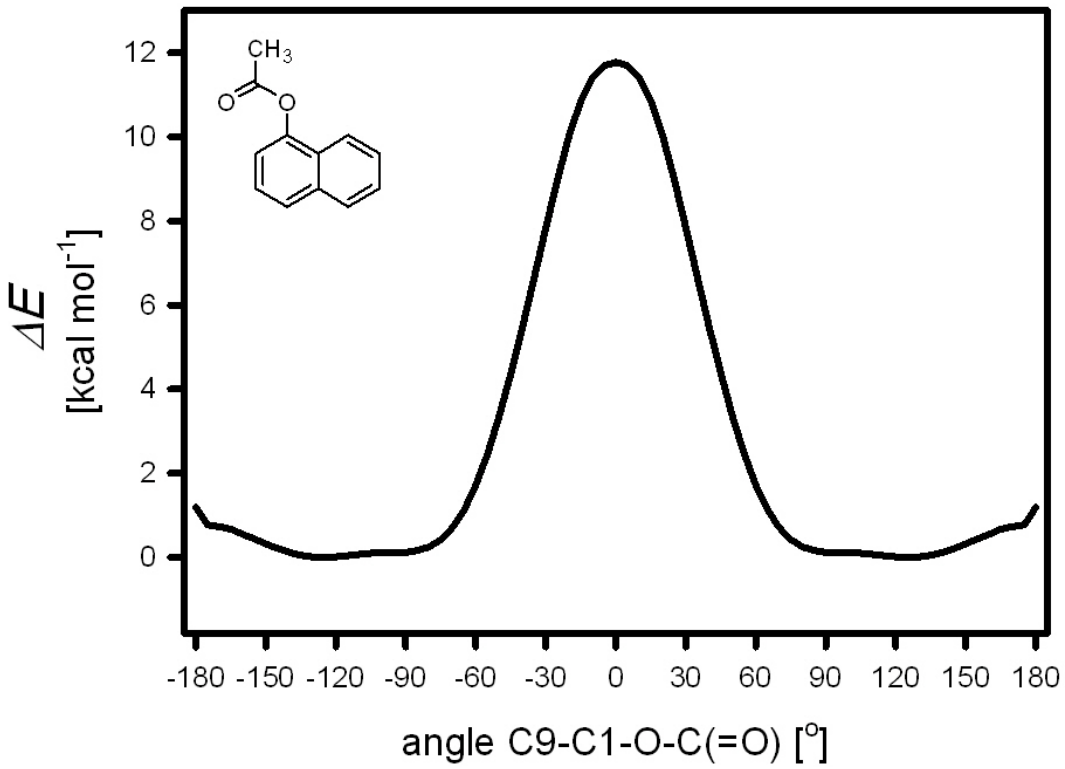

Figure SC8. Energy profile for rotation of C-O bond in *O*-acetylo-1-naphthol calculated at the LC-wPBE/6-311++G(d,p) level.

Copies of ^{1}H and ^{13}C NMR spectra